

## **Homeodomain-interacting protein kinase 2 regulates DNA damage response through interacting with heterochromatin protein 1 $\gamma$**

Yoko Akaike, Yuki Kuwano, Kensei Nishida, Ken Kurokawa, Keisuke Kajita, Shizuka Kano,  
Kiyoshi Masuda, and Kazuhito Rokutan \*

*Department of Stress Science, Institute of Health Biosciences, Tokushima University Graduate  
School, Tokushima 770-8503, Japan*

The running title: HP1 $\gamma$  as a novel target for HIPK2.

\*Corresponding author: Kazuhito Rokutan, MD., PhD.

Department of Stress Science, Institute of Health Biosciences

Tokushima University Graduate School

3-18-15 Kuramoto-cho, Tokushima 770-8503, Japan

Phone: +81-88-633-9007, Fax: +81-88-633-9008

E-mail: [rokutan@tokushima-u.ac.jp](mailto:rokutan@tokushima-u.ac.jp)

**ABSTRACT**

**Homeodomain-interacting protein kinase 2 (HIPK2) is a potential tumor suppressor that plays a crucial role in the DNA damage response (DDR) by regulating cell cycle checkpoint activation and apoptosis. However, it is unclear whether HIPK2 exerts distinct roles in DNA damage repair. The aim of this study was to identify novel target molecule(s) of HIPK2, which mediates HIPK2-dependent DNA damage repair.**

**HIPK2-knockdown human colon cancer cells (HCT116) or *hipk1/hipk2* double-deficient mouse embryonic fibroblasts could not remove histone H2A.X phosphorylated at Ser139 ( $\gamma$ H2A.X) after irradiation with a sublethal dose (10 J/m<sup>2</sup>) of ultraviolet (UV)-C, resulting in apoptosis. Knockdown of HIPK2 in p53-null HCT116 cells similarly promoted the UV-C-induced  $\gamma$ H2A.X accumulation and apoptosis. Proteomic analysis of HIPK2-associated proteins using liquid chromatography-tandem mass spectrometry identified heterochromatin protein 1 $\gamma$  (HP1 $\gamma$ ) as a novel target for HIPK2.**

**Immunoprecipitation experiments with HCT116 cells expressing FLAG-tagged HIPK2 and one of the HA-tagged HP1 family members demonstrated that HIPK2 specifically associated with HP1 $\gamma$ , but not with HP1 $\alpha$  or HP1 $\beta$ , through its chromo-shadow domain. Mutation of the HP1box motif (883-PTVSV-887) within HIPK2 abolished the association. HP1 $\gamma$  knockdown also enhanced accumulation of  $\gamma$ H2A.X and apoptosis after sublethal UV-C irradiation. *In vitro* kinase assay demonstrated an HP1 $\gamma$ -phosphorylating activity of HIPK2. Sublethal UV-C irradiation phosphorylated HP1 $\gamma$ . This phosphorylation was absent in endogenous HIPK2-silenced cells with HIPK2 3'UTR siRNA.**

**Overexpression of FLAG-HIPK2, but not the HP1box-mutated or kinase-dead HIPK2 mutant, in the HIPK2-silenced cells increased HP1 $\gamma$  binding to trimethylated (Lys9) histone H3 (H3K9me3), rescued the UV-C-induced phosphorylation of HP1 $\gamma$ , triggered release of HP1 $\gamma$  from histone H3K9me3, and suppressed  $\gamma$ H2A.X accumulation. Our**

**results suggest that HIPK2-dependent phosphorylation of HP1 $\gamma$  may participate in the regulation of dynamic interaction between HP1 $\gamma$  and histone H3K9me3 to promote DNA damage repair. This HIPK2/HP1 $\gamma$  pathway may uncover a new functional aspect of HIPK2 as a tumor suppressor.**

**KEYWORDS:** DNA damage response; HIPK2; HP1 $\gamma$ ; chromatin remodeling; DNA damage repair

## INTRODUCTION

Genome integrity is constantly threatened by environmental agents and by metabolic products that can cause DNA damage. To counteract these threats, eukaryotic cells rely on a coordinated series of events termed the DNA damage response (DDR), which allows DNA damage detection, cell-cycle checkpoint activation, and DNA damage repair.<sup>1</sup> DDR provides a potent innate barrier against cellular transformation and tumorigenesis.

Homeodomain-interacting protein kinase 2 (HIPK2) is a DNA damage-responsive kinase that phosphorylation-dependently activates the apoptotic program through interacting with diverse downstream targets including tumor suppressor p53 (ref. 2, 3). In unstressed cells, HIPK2 is constantly degraded by the ubiquitin-proteasome system.<sup>4</sup> Genotoxic stress, such as ultraviolet (UV) light, drugs, or ionizing radiation (IR), stabilizes HIPK2 through dissociation of an E3 ubiquitin ligase Siah-1, Siah-2, WSB-1, or MDM2 (ref. 2, 3). At the same time, genotoxic stress activates HIPK2 through caspase-6-mediated cleavage of its C-terminal auto-inhibitory domain or by auto-phosphorylation at an activation loop in its kinase domain.<sup>5</sup>

<sup>6</sup> It is also important to note that HIPK2 functions differently depending on the severity of DNA damage. Upon apoptosis-inducing, lethal DNA damage, HIPK2 phosphorylates p53 at Ser46 and induces apoptosis.<sup>7, 8</sup> In addition, HIPK2 promotes p53-independent apoptosis through interacting with CtBP, Daxx, or  $\Delta p63\alpha$ .<sup>9</sup> In contrast, when DNA damage has less impact for cells, damaged DNA is repaired by the DNA repair system in association with cell cycle arrest needed for the repair. In this case, HIPK2 does not phosphorylate p53 at Ser46 (ref. 4). Instead, HIPK2 mediates p53 recruitment onto the *CDKN1A* promoter through acetylation of p53 by p300/CBP-associated factor to induce cell cycle arrest.<sup>10</sup> Thus, HIPK2 plays an important role in DDR by regulating cell cycle arrest and apoptosis for prevention of mutations, genome instability, and carcinogenesis. Compared to these well-known functions in DDR, it is still unclear whether HIPK2 exerts distinct roles in DNA damage repair.

Recently, HIPK2 has been suggested to function as an epigenetic regulator of chromatin structure. HIPK2 interacts with methyl-CpG-binding protein MeCP2, methyl-binding transcription factor ZBTB4, chromosomal protein HMGA1, transcriptional corepressor CtBP, and polycomb protein Pc2 (ref. 9). Chromatin components and epigenetic factors regulate the integrated response of chromatin for promoting DNA damage signaling and repair.<sup>11, 12</sup> It is possible to speculate that HIPK2 may regulate the organization of chromatin structure to control gene transcription or DNA repair. However, the contribution of HIPK2 to chromatin remodeling has not been fully documented.

In this study, we identified heterochromatin protein 1 $\gamma$  (HP1 $\gamma$ ) as a novel target for HIPK2. HP1 $\gamma$  is a member of the HP1 family that consists of HP1 $\alpha$ , HP1 $\beta$ , and HP1 $\gamma$ .<sup>13</sup> HP1 proteins are heterochromatin component factors that regulate chromatin structure.<sup>14</sup> HP1 proteins bind to histone H3 dimethylated or trimethylated at Lys9 (histone H3K9me2 and histone H3K9me3, respectively) through its N-terminal chromo domain and interact with other HP1 isoforms through its C-terminal chromo-shadow domain to facilitate heterochromatin formation for gene silencing.<sup>15</sup> Moreover, HP1 interacts with a number of chromatin modifying proteins including transcription-associated proteins, DNA replication and repair proteins, and RNA-associated proteins through its chromo-shadow domain.<sup>16</sup> Although HP1 family proteins share several target proteins, individual HP1 proteins target different proteins and possess distinct functions.<sup>16</sup> Recently, studies have focused on elucidating how HP1 proteins participate in DDR.<sup>17-20</sup> In several studies, HP1 proteins are released from histone H3K9me3 and promote recruitment of DDR factors to damaged sites for DNA repair.<sup>17</sup> On the other hand, all HP1 proteins are recruited to DNA damage sites after being released from chromatin.<sup>19</sup> These reports suggest that HP1 proteins may regulate chromatin structure through changing their affinity to chromatin in response to DNA damage and promote repair of damaged DNA.

The present study revealed that HIPK2 specifically bound to and phosphorylated HP1 $\gamma$  in response to sublethal UV-C irradiation in human colon cancer cells (HCT116), facilitating dissociation of HP1 $\gamma$  from histone H3K9me3. Moreover, HIPK2 knockdown impaired removal of damaged DNA byproducts or phosphorylated (Ser139) histone H2A.X ( $\gamma$ H2A.X) and facilitated apoptotic cell death. Our results may disclose a novel HIPK2-mediated pathway for DDR through interacting with HP1 $\gamma$ .

## RESULTS

### *Reduction of HIPK2 induces apoptosis after sublethal UV-C irradiation*

To confirm an important role of HIPK2 in protection against DNA damage, HCT116 cells were transfected with two different small-interfering (si) RNAs (#1 and #2) targeting *HIPK2* (ref.21) for 48 h and then exposed to irradiation with 10 J/m<sup>2</sup> UV-C. The two independent siRNAs efficiently reduced *HIPK2* mRNA (Supplementary Figure S1a). However, as noted by others,<sup>22</sup> we could not detect endogenous HIPK2 protein using any commercially available antibodies. We therefore transfected with pCMV-3FLAG-tagged HIPK2 (FLAG-HIPK2) and confirmed that HIPK2 siRNAs efficiently knocked down FLAG-HIPK2 (Supplementary Figure S1b). As previously reported,<sup>4</sup> exposure of HCT116 cells to 10 J/m<sup>2</sup> UV-C irradiation did not induce phosphorylation of p53 at Ser46 and did not activate caspase-3 (Supplementary Figure S2); this dose was thus considered to be sublethal. In HCT116 cells treated with HIPK2 siRNA#1 or #2, 10 J/m<sup>2</sup> UV-C increased the numbers of terminal deoxynucleotidyltransferase-mediated UTP end labeling (TUNEL)-positive cells (Figure 1a) in association with processing of caspase-9 and caspase-3 (Figure 1b). Consequently, the irradiation significantly decreased viability of HIPK2-knockdown cells (Figure 1c). In contrast, none of these cellular events occurred in control siRNA-treated cells (Figure 1a-c). These results suggested an important role of HIPK2 in protection against damage caused by sublethal UV-C irradiation. We used HIPK2 siRNA#1 to reduce HIPK2 in the following experiments.

### *Reduction of HIPK2 impairs DNA damage repair*

UV light forms three major classes of DNA lesions; (6-4) photoproducts (6-4PPs), cyclobutane pyrimidine dimers, and their Dewar isomers, which are removed by the nucleotide excision repair system.<sup>23</sup> HIPK2 or control siRNA-treated cells were exposed to 10

J/m<sup>2</sup> UV-C, and time-dependent changes in 6-4PP levels were measured using an enzyme-linked immunosorbent assay (ELISA). As shown in Figure 2a, control siRNA-treated cells removed about 80% of the initial 6-4PPs within 3 h after finishing UV-C irradiation, while HIPK2-knockdown cells removed only 10% of 6-4PPs within 3 h after UV-C irradiation, and significantly higher levels of 6-4PPs remained to be accumulated. The remaining photoproducts induce double-strand breaks (DSBs), and surrounding histone H2A.X is phosphorylated at Ser139 ( $\gamma$ H2A.X) to initiate recruitment of DNA repair factors to damaged DNA sites.  $\gamma$ H2A.X is targeted for dephosphorylation following repair, and its removal is key for allowing restoration of the epigenome to the pre-damage status.<sup>24</sup> Although  $\gamma$ H2A.X is not a specific marker for DSBs, it can be used to measure the kinetics of DNA repair.<sup>25,26</sup> As shown in Figure 2b, HIPK2 knockdown significantly enhanced the UV-C-induced accumulation of  $\gamma$ H2A.X, compared with that in control siRNA-treated cells.

The HIPK family consists of three members (HIPK1, HIPK2, and HIPK3).<sup>27</sup> The functional importance of HIPKs has mainly been studied using HIPK2. HIPK1 and HIPK2 are suggested to have overlapping roles in mediating cell proliferation or apoptosis in response to morphogenetic and genotoxic signals.<sup>28</sup> To test whether HIPK2 participates in the DNA damage repair response, we compared the time-dependent resolution of  $\gamma$ H2A.X after irradiation with 5 J/m<sup>2</sup> UV-C between wild-type and *hipk1/hipk2* double-deficient mouse embryonic fibroblasts (*hipk1*<sup>-/-</sup>*hipk2*<sup>-/-</sup> MEFs) (kindly provided by Dr. Isono).

$\gamma$ H2A.X-positive cells (> 10  $\gamma$ H2A.X foci in a cell) appeared within 1 h after the irradiation similarly in both wild-type and *hipk1*<sup>-/-</sup>*hipk2*<sup>-/-</sup> MEFs (Figure 2c). Although  $\gamma$ H2A.X-positive cells decreased time-dependently in wild-type MEFs, *hipk1*<sup>-/-</sup>*hipk2*<sup>-/-</sup> MEFs could not remove  $\gamma$ H2A.X, and numbers of  $\gamma$ H2A.X-positive cells were rather increased 3 and 24 h after the UV-C irradiation (Figure 2c).

We also examined whether p53 was needed for the HIPK2-mediated protection against



sublethal UV-C irradiation using p53-null (p53<sup>-/-</sup>) HCT116 cells (provided by De.Vogelstein). The absence of p53 did not cause accumulation of  $\gamma$ H2A.X or activation of caspase-3 and did not change cell viability after irradiation with 10 J/m<sup>2</sup> UV-C (Supplementary Figure S3a-c). Similarly observed in wild-type p53-expressing cells, silencing of HIPK2 in p53<sup>-/-</sup> cells promoted the UV-C-induced  $\gamma$ H2A.X accumulation and caspase-3 activation. Consequently, apoptosis was induced even in the absence of p53 (Supplementary Figure S3a-c).

#### *HIPK2 associates with HP1 $\gamma$*

HIPK2 interacts with numerous target proteins in a variety of biological processes.<sup>29</sup> We next attempted to identify new HIPK2 target proteins that might be involved in DNA repair responses. HCT116 cells were transfected with a vector encoding FLAG-HIPK2 or an empty vector (FLAG-mock) for 48 h. Nuclear proteins were immunoprecipitated with an anti-FLAG antibody, separated by sodium dodecyl sulfate-polyacrylamide gel electrophoresis (SDS-PAGE), and subjected to silver staining. A number of HIPK2-associated proteins were immunoprecipitated (Figure 3a). We surveyed HIPK2 targets reported and focused on the 22 kDa protein band, since any interacting partner with a molecular mass of 22 kDa has not been reported. Analysis of the 22-kDa protein band using liquid chromatography-tandem mass spectrometry (LC-MS/MS) identified HP1 $\gamma$  as a possible downstream effector of HIPK2.

To confirm the specific association between HIPK2 and HP1 $\gamma$ , we first examined the interaction between HIPK2 and three HP1 family members using HCT116 cells overexpressing FLAG-HIPK2. FLAG-HIPK2 associated with endogenous HP1 $\gamma$ , but not with HP1 $\alpha$  or HP1 $\beta$  (Figure 3b). Next, FLAG-HIPK2 and one of the pcDNA3.1(-)-C-terminal HA-tagged HP1 family members (HA-HP1 $\alpha$ , HA-HP1 $\beta$ , or HA-HP1 $\gamma$ ) were overexpressed in HCT116 cells, and prepared nuclear proteins were subjected to immunoprecipitation with an anti-HA antibody. As shown in Figure 3c, FLAG-HIPK2 was detected only in

immunoprecipitates prepared from HA-HP1 $\gamma$ -expressing cells. The association between HIPK2 and HP1 $\gamma$  was also found in p53<sup>-/-</sup> HCT116 and human embryonic kidney cells (HEK293T) (Figure 3d and e).

HP1 partners possess a conserved PxVxL/M/V pentapeptide motif called HP1box, which is necessary and sufficient for their interaction with HP1.<sup>30</sup> HP1 $\gamma$  possesses two HP1box motifs (525-PFVTM-529 and 883-PTVSV-887) (Figure 3f). Mutation of the 883-PTVSV-887 (HIPK2mt2), but not the 525-PFVTM-529 (HIPK2mt1), blocked the interaction between HIPK2 and HP1 $\gamma$  (Figure 3f). Thus, HP1 $\gamma$  was likely to be one of the important downstream effectors of HIPK2. Using HCT116 cells co-transfected with the FLAG-HIPK2-encoding vector and the vector encoding either HA-HP1 $\gamma$ , HA-HP1 $\gamma$  lacking the chromo domain (HA- $\Delta$ CD), or HA-HP1 $\gamma$  lacking the chromo-shadow domain (HA- $\Delta$ CSD) (Supplementary Figure S4a), we confirmed that the chromo-shadow domain of HP1 $\gamma$  was responsible for the association between HIPK2 and HP1 $\gamma$  (Supplementary Figure S4b).

#### *HIPK2 phosphorylates HP1 $\gamma$*

HIPK2 exerts its functions through phosphorylating target proteins.<sup>29</sup> HP1 $\gamma$  also undergoes extensive phosphorylation, but distinct kinase-mediated phosphorylation events and their specific roles are poorly understood.<sup>31</sup> HIPK2 phosphorylates target proteins having serine or threonine just before or after proline (S/T-P or P-S/T).<sup>32</sup> On the other hand, HIPK2 phosphorylates  $\beta$ -catenin and histone H2B, which do not have these canonical phosphorylation sites.<sup>33, 34</sup> HP1 $\gamma$  also does not have either of the canonical phosphorylation sites (Supplementary Figure S5a).

To test the possibility that HIPK2 might mediate the phosphorylation of HP1 $\gamma$ , first we employed *in vitro* kinase assays. After transfection with the vector encoding either FLAG-HIPK2 or FLAG-tagged kinase-dead HIPK2 mutant (FLAG-HIPK2-KD), or an empty

vector, FLAG-HIPK2 and FLAG-HIPK2-KD were immunopurified and incubated with recombinant HP1 $\gamma$  in the presence of  $\gamma^{32}$ P-ATP. As shown in Figure 4a, wild-type FLAG-HIPK2, but not FLAG-HIPK2-KD, was able to phosphorylate HP1 $\gamma$  and HIPK2 itself.

Phos-tag SDS-PAGE demonstrated that sublethal UV-C irradiation phosphorylated HP1 $\gamma$  (Supplementary Figure S5b). We examined whether HIPK2 participated in this UV-C-induced phosphorylation. First, we confirmed that the reduction of endogenous HIPK2 with a siRNA targeting HIPK2 3'UTR (HIPK2 3'U siRNA, Supplementary Figure S1a and c) inhibited the UV-C-induced phosphorylation of HP1 $\gamma$  in mock-transfected control cells (Figure 4b and c). Next, we examined whether overexpressed FLAG-HIPK2 could rescue the phosphorylation activity, and found that FLAG-HIPK2 phosphorylated HP1 $\gamma$  in response to UV-C in HIPK2 3'U siRNA-treated cells (Figure 4b and c). In contrast, FLAG-HIPK2-KD-overexpressing cells could not fully phosphorylate HP1 $\gamma$  after UV-C irradiation (Figure 4b and c). These results suggest that HIPK2 may participate in the UV-C-induced phosphorylation of HP1 $\gamma$ . Moreover, we found that the overexpression of FLAG-HIPK2, but not FLAG-HIPK2-KD, significantly suppressed the UV-C-induced accumulation of  $\gamma$ H2A.X in the HIPK2-silenced cells (Figure 4d).

Using cells overexpressing HA-HP1 $\gamma$  or truncated HA-HP1 $\gamma$  lacking the chromo domain or the chromo-shadow domain, we showed that the chromo-shadow domain was likely to possess the phosphorylation sites. We also confirmed that overexpression of FLAG-HIPK2mt2, which could not bind to HP1 $\gamma$ , did not stimulate the UV-C-induced phosphorylation of HP1 $\gamma$  (Supplementary Figure S5d). HP1 $\gamma$  at Ser83 was already identified as the phosphorylation site of protein kinase A and Aurora kinase A,<sup>35, 36</sup> while sublethal UV-C irradiation did not phosphorylate HP1 $\gamma$  at Ser83 (Supplementary Figure S5e).

*HIPK2 regulates association between HP1 $\gamma$  and histone H3K9me3*

HIPK2 reduces protein levels of the epigenetics-associated proteins, CtBP and ZBTB4 (ref. 32, 37), through stimulating the ubiquitin-proteasome system. In the case of HP1 $\gamma$ , neither reduction nor overexpression of HIPK2 changed HP1 $\gamma$  protein levels (Supplementary Figure S6a and b). We also confirmed a crucial role of HP1 $\gamma$  in DNA damage repair response; HP1 $\gamma$  knockdown (Figure 5a) augmented  $\gamma$ H2A.X accumulation (Figure 5b) and activated caspase-3 (Figure 5c) in response to 10 J/m<sup>2</sup> UV-C.

We next examined whether HIPK2 regulated the binding of HP1 $\gamma$  to histone H3K9me3 and chromatin. After endogenous HIPK2 was silenced with HIPK2 3'U siRNA, we examined how FLAG-HIPK2, -HIPK2mt2 or -HIPK2-KD affected the binding of HP1 $\gamma$  to histone H3K9me3 before and after exposure to UV-C. Immunoprecipitation experiments with an anti-histone H3K9me3 showed that HA-HP1 $\gamma$  did not significantly associate with histone H3K9me3 before and after UV-C exposure when endogenous HIPK2 was reduced with HIPK2 3'U siRNA (Figure 6a). It should be noted that overexpression of FLAG-HIPK2 increased HA-HP1 $\gamma$  binding to histone H3K9me3, and that UV-C triggered the release of HA-HP1 $\gamma$  from histone H3K9me3 (Figure 6a). Overexpression of the HP1box mutant (FLAG-HIPK2mt2) did not trigger the interaction between HA-HP1 $\gamma$  and histone H3K9me3 (Figure 6a). Overexpression of the kinase-dead mutant of HIPK2 (FLAG-HIPK2-KD) also impaired the association of HA-HP1 $\gamma$  with histone H3K9me3 and failed to release of HA-HP1 $\gamma$  from histone H3K9me3 after UV-C irradiation (Figure 6a).

The chromatin fractionation assay was also performed after HCT116 cells were transfection with the vector encoding FLAG-HIPK2, FLAG-HIPK2mt2, or FLAG-HIPK2-KD. Although HP1 $\gamma$  mainly associated with chromatin, overexpressed FLAG-HIPK2 significantly increased the distribution of HP1 $\gamma$  in soluble fractions in response to UV-C (Figure 6b). This UV-C-induced response of HP1 $\gamma$  was not observed in FLAG-HIPK2mt2- or FLAG-HIPK2-KD-expressing cells (Figure 6b). As also shown in

Figure 6b, significant HIPK2-dependent changes in the distribution of HP1 $\alpha$  and HP1 $\beta$  were not observed before and after exposure to UV-C. We also confirmed that UV-C irradiation did not modify the interaction between HIPK2 and HP1 $\gamma$  (Supplementary Fig. S6c).

## DISCUSSION

HIPK2 is a potential tumor suppressor that plays a fundamental role in apoptosis induction upon severe DNA damage by phosphorylating p53 at Ser46 and CtBP at Ser422 (ref. 2, 3). HIPK2 is also stabilized in response to sublethal DNA damage, when p53 Ser46 phosphorylation, CtBP degradation, and apoptosis induction are absent. This suggests an additional, non-apoptotic role of HIPK2. In this study, we have identified HP1 $\gamma$  as a novel target for HIPK2 and suggest that the interaction between HIPK2 and HP1 $\gamma$  may constitute a part of an integrated response to promote the DNA damage repair in response to sublethal DNA damage. Knockdown of HIPK2 as well as HP1 $\gamma$  impaired the removal of accumulated 6-4PPs and  $\gamma$ H2A.X after exposure to sublethal UV-C irradiation, leading to apoptotic cell death. We also showed that *hipk1*<sup>-/-</sup>*hipk2*<sup>-/-</sup> MEFs could not remove UV-C-induced  $\gamma$ H2A.X, but time-dependently increased  $\gamma$ H2A.X foci. Our results may uncover a new HIPK2-dependent pathway for the DNA damage repair and possibly for chromatin remodeling. This pathway may play an important role in HIPK2-mediated prevention of mutations, genome instability, and carcinogenesis.

HIPK2 up-regulates the expression of a p53-inducible DNA repair factor p53R2 after sublethal UV irradiation or Adriamycin treatment.<sup>38</sup> p53R2 is required for maintenance of mitochondrial DNA and for optimal DNA repair after UV damage,<sup>39</sup> suggesting a possible role of HIPK2 in DNA repair responses. However, the *RRM2B* gene encoding p53R2 is inactivated due to a point mutation in HCT116 cells.<sup>40</sup> Furthermore, using p53<sup>-/-</sup> HCT116 cells, we demonstrated that the absence of p53 did not cancel the HIPK2-dependent protection against damage after sublethal UV-C irradiation. We also found that HIPK2 could associate with HP1 $\gamma$  even in the p53-null cells. Recently, it has been shown that HIPK2 constitutively phosphorylates WIP1 (wild-type p53-induced phosphatase 1) and facilitates the proteasomal degradation of WIP1 in unstressed cells.<sup>41</sup> This HIPK2-mediated down-regulation of WIP1

levels is crucial for the initiation of the DSB repair signaling pathway; reduction of HIPK2 inhibits IR-induced  $\gamma$ H2A.X foci formation, cell-cycle checkpoint activation, and DNA repair signaling.<sup>41</sup> In our experiments, however, HIPK2-knockdown cells failed to remove UV-C-induced 6-4PPs and rather enhanced  $\gamma$ H2A.X foci formation, leading to p53-independent apoptosis. Besides the p53R2- or WIP1-mediated regulation, our results suggest the presence of another HIPK2-dependent, p53-independent pathway for DDR through interacting with HP1 $\gamma$ .

Sublethal UV-C irradiation phosphorylated HP1 $\gamma$ . This UV-C-induced phosphorylation did not occur after reduction of endogenous HIPK2 with HIPK2 3'UTR siRNA, and overexpressed HIPK2, but not kinase-dead HIPK2, fully rescued the phosphorylation activity. Moreover, HIPK2 contains two conserved pentapeptide motifs (525-PFVTM-529 and 883-PTVSV-887) called HP1box, which is necessary and sufficient for their interaction with HP1.<sup>30</sup> Mutation of the 883-PTVSV-887 to the 883-PT $\underline{A}$ SV-887 impaired not only the association between HIPK2 and HP1 $\gamma$ , but also inhibited the UV-C-induced phosphorylation of HP1 $\gamma$ . These results suggest that HP1 $\gamma$  is an important downstream effector of HIPK2 in the response to UVC.

In response to DNA damage, chromatin becomes remodeled to facilitate access of the DDR machinery to the sites of damage.<sup>1,12</sup> However, the chromatin rearrangements taking place in response to DNA damage are not fully understood. It is also unknown whether and how HIPK2 affects chromatin remodeling, although several epigenetics-related proteins have been identified as HIPK2-interacting partners.<sup>9</sup> Recently, several lines of evidence have revealed that HP1 proteins dynamically associate and dissociate with chromatin to play an active role in DNA damage repair processes.<sup>17,19,20,42</sup> In addition, HP1 proteins co-localize with  $\gamma$ H2A.X or DDR factors, such as DDB2, XPA, and PCNA.<sup>19,43</sup> However, the spatial and temporal regulation of the association and dissociation of HP1 proteins with chromatin in response to

DNA damage is not fully understood. Moreover, the specific contributions of each HP1 subtype to the DDR signaling and DSB repair pathways are not clearly understood. HP1 $\alpha$  is recruited to damaged sites depending on the large subunit of chromatin assembly factor-1 (p150CAF-1) and leads to accumulation of p53 foci at DNA damage sites, where it promotes homologous recombination repair.<sup>42</sup> More recently, Lee *et al.* have shown that HP1-mediated recruitment of BRCA1 (breast cancer susceptibility gene 1) is crucial for the BRCA1-dependent homologous recombination repair and the arrest of cell cycle at the G<sub>2</sub>/M checkpoint.<sup>18</sup> Although all three subtypes of the HP1 family seemed to be equally important for the DDR signaling and DSB repair pathway, Lee *et al.* suggested non-redundant roles of three HP1 subtypes in DDR pathway; silencing of HP1 $\gamma$  more prominently caused IR-induced apoptosis, compared with silencing of the other subtypes.<sup>18</sup> We show here that HIPK2 associates specifically with HP1 $\gamma$ , but not with HP1 $\alpha$  or HP1 $\beta$ . Among the HP1 family members, only HP1 $\gamma$  associates with both heterochromatin and euchromatin.<sup>44</sup> Euchromatic regions are thought to be more susceptible to DNA damage. Several studies indicate that  $\gamma$ H2A.X foci preferentially assemble in euchromatin or are predominantly located at the boundary of heterochromatin,<sup>45-47</sup> and the actual DSB repair is carried out within euchromatin.<sup>48,49</sup> Considering those findings, HIPK2/HP1 $\gamma$  may be one of the crucial pathways for DNA repair reactions. Along with this line, our results suggest that HIPK2 may regulate the dynamic interaction between HP1 $\gamma$  and histone H3K9me3.

Phosphorylation of HP1 proteins regulates their binding to chromatin in response to DNA damage.<sup>50</sup> Casein kinase 2-mediated phosphorylation of HP1 $\beta$  at Thr51 causes release of this protein from histone H3K9me3 (ref. 17). Phosphorylation of HP1 $\alpha$  at Ser11-14 rather increases the affinity of HP1 $\alpha$  for histone H3K9me.<sup>51</sup> Although HP1 $\gamma$  does not have any canonical phosphorylation sites for HIPK2, *in vitro* kinase assays demonstrated the HP1 $\gamma$ -phosphorylating ability of HIPK2. Overexpression of FLAG-HIPK2 in HIPK2-silenced



cells with HIPK2 3'UTR siRNA increased HP1 $\gamma$  binding to histone H3K9me3. Overexpressed FLAG-HIPK2 not only rescued the ability to phosphorylate HP1 $\gamma$ , but also triggered release of HP1 $\gamma$  from histone H3K9me3, when exposed to UV-C. Overexpression of the HP1box mutant (883-PTASV-887) or kinase-dead mutant of HIPK2 in the HIPK2-silenced cells impaired the HP1 $\gamma$  binding to histone H3K9me3 and did not initiate the release of HP1 $\gamma$  from histone H3K9me3 in response to UV-C. Consequently, UV-C-induced release of HP1 $\gamma$  from chromatin after UV-C irradiation could be detected in cells overexpressing FLAG-HIPK2, but not the HP1box mutant or the kinase-dead mutant. These results suggest that HIPK2-dependent phosphorylation of HP1 $\gamma$  may at least in part regulate the dynamic interaction between HP1 $\gamma$  and histone H3K9me3 for DNA damage repair. To definitively prove that HP1 $\gamma$  is an important downstream effector of HIPK2 in the response to UV-C, the specific sites by which HIPK2 phosphorylates HP1 $\gamma$  should be identified. The chromo-shadow domain seems to possess the phosphorylation site(s). Further studies are needed to identify the site(s).

## MATERIALS AND METHODS

### *Cell culture and siRNA experiments*

HCT116, HEK293T, and MEF cells were cultured in recommended media supplemented with 5% or 10% (v/v) FCS. Wild-type and *hipk1*<sup>-/-</sup>*hipk2*<sup>-/-</sup> MEFs were kindly provided by Dr. Isono.<sup>28</sup> We used siRNAs targeting HIPK2 (#1, 5'-CGAAGCACUGUGAGCCUCCUUGAUA-3'; #2, 5'-UCUCCAUAACUAAACUACCCAUCUAC-3'),<sup>21</sup> HIPK2 3'UTR (5'-AACAAUGUCUCUCAAUGGGGAAGG-3') (Invitrogen, Carlsbad, CA), or HP1 $\gamma$  (5'-AAGAGGCAGAGCCTGAAGAAT-3') (Qiagen, Hilden, Germany). Stealth RNAi negative control (Invitrogen) was used as a control siRNA. Cells were treated with the indicated siRNAs at a final concentration of 10 nM using Lipofectamine RNAiMAX (Invitrogen) according to the manufacturer's protocol.

### *UV-C irradiation, measurements of 6-4PPs and apoptosis*

After cells were irradiated with UV-C using a UV crosslinker (UVP, Upland, CA), numbers of viable cells were counted using an automatic cell counter (Invitrogen). TUNEL analysis was employed to quantify apoptosis using the DeadEnd colorimetric TUNEL system (Promega, Madison, WI) according to the manufacturer's protocol. Genomic DNAs were isolated from cells using Nucleospin tissue (Takara, Otsu, Japan), and 6-4PPs were quantified by an OxiSelect UV-Induced DNA Damage ELISA Kit (Cell Biolabs, San Diego, CA) according to the manufacturer's protocols.

### *Construction of plasmids*

pCMV-3FLAG-tagged HIPK2 vector was generated as previously described.<sup>21</sup>

FLAG-HIPK2-KD, which contains a mutation in the ATP-binding site of the kinase domain

(Lys to Ala at position 228 [NP\_073577.3]), was prepared from pCMV-3FLAG-tagged HIPK2 vector using the KOD-Plus-Mutagenesis Kit (TOYOBO, Osaka, Japan).<sup>27</sup> Two HP1-binding PxVxL/M/V motifs in HIPK2 were mutated (Val527 to Ala and Val885 to Ala) and subcloned into pCMV-3FLAG-tagged vector (FLAG-HIPK2mt1 and FLAG-HIPK2mt2, respectively). A human cDNA library was generated from HCT116 cells, and *HP1*  $\alpha$ , *HP1*  $\beta$ , and *HP1*  $\gamma$  cDNAs were amplified by PCR using the following primer sets;

5'-AAAACTCGAGCACCATGGGAAAGAAAACCAAGCGGACAGCTGACAGTTCTTCTTCAGAGGATGA-3' (forward; *Xho*I site is underlined) and

5'-AAAAGGATCCTTAAAGCGTAATCCGGAACATCGTATGGGTACATGCTCTTTGCTGTTCCTT-3' (reverse; *Bam*HI site is underlined) for *HP1*  $\alpha$ ,

5'-AAAAGATATCATGGGGAAAAACAAAACAAGAAGAAAGTGGAGGAGGTGCTAGAAGAGGA-3' (forward; *Eco*RV site is underlined) and

5'-AAAAGGATCCTTAAAGCGTAATCCGGAACATCGTATGGGTACATGTTCTTGTCATCTTTT-3' (reverse; *Bam*HI site is underlined) for *HP1*  $\beta$ , and

5'-AAAAGATATCATGGCCTCCAACAAAACACTACATTGCAAAAAATGGGAAAAAAACAGAATGG-3' (forward; *Eco*RV site is underlined) and

5'-AAAAGGATCCTTAAAGCGTAATCCGGAACATCGTATGGGTACATTTGAGCTTCATCTTCTG-3' (reverse; *Bam*HI site is underlined) for *HP1*  $\gamma$ . The amplified products were cloned

into the mammalian expression vector pcDNA3.1 (-) (Invitrogen). HA was appended to C-termini of these insert sequences. *HP1*  $\gamma$  deletion mutants were generated by PCR using

HA-tagged *HP1*  $\gamma$  as a template. Human *HP1*  $\gamma$  was amplified by PCR using the primers

5'-AAAAGGATCCATGGCCTCCAACAAAACACTAC-3' (forward; *Bam*HI site is underlined)

and 5'-AAAACTCGAGTTATTGAGCTTCATCTTCTG-3' (reverse; *Xho*I site is underlined),

and cloned into the pGEX-6p-1 vector (GE Healthcare, Piscataway, NJ). All constructs were

confirmed to have the expected sequence by DNA sequencing. Plasmids were then transfected

using Fugene HD (Promega) according to the manufacturer's instructions.

#### *Quantitative real-time RT-PCR (qPCR)*

Total RNAs were extracted from cells using an RNAiso plus (Takara). One microgram of isolated RNA was reverse-transcribed using ReverTra Ace reverse transcriptase (TOYOBO). Target mRNA levels were measured using SYBR green master mix and an ABI 7500 real-time system (Applied Biosystems, Foster City, CA). *Glyceraldehyde 3-phosphate dehydrogenase (GAPDH)* mRNA was measured as an internal control for normalization. The data are presented as fold changes in gene expression relative to controls measured in control siRNA-treated cells. The following primer sets were used for *HIPK2* (forward, 5'-AGCAGCACCAGTCATCTGTG-3' and reverse, 5'-GGAGCTGATGGCCTGAGA-3')<sup>21</sup>, for *HPI1 $\gamma$*  (forward, 5'-TTGCCAGAGGTCTTGATCC-3' and reverse, 5'-TGCCTCATCTGAATCTTTCCAT-3'), and for *GAPDH* (forward, 5'-AGCCACATCGCTCAGACAC-3' and reverse, 5'-GCCCAATACGACCAAATCC-3').

#### *Subcellular fractionation*

After washing with phosphate-buffered saline (PBS), cells were lysed in RIPA buffer (Cell Signaling Technology, Danvers, MA) containing a protease inhibitor cocktail (Promega) and a phosphatase inhibitor cocktail (Roche Applied Science, Indianapolis, IN). Whole-cell extracts were collected by centrifugation at 20,000 g for 15 min at 4°C. Nuclear fractionation was done as previously described.<sup>52</sup> The chromatin fractionation assay was performed as described by Mund *et al.*<sup>53</sup> with minor modifications. Soluble proteins were extracted with E1A buffer (50 mM HEPES, pH 8.0, containing 150 mM NaCl and 0.1% NP-40) for 25 min on ice and were then centrifuged at 16,100 g for 15 min at 4°C. Supernatants were collected as soluble protein fractions. After the pellets were washed with PBS, chromatin-bound proteins were

extracted from the pellets in a chromatin extraction buffer (50 mM HEPES, pH 8.0, containing 400 mM NaCl, 2.5 mM MgCl<sub>2</sub>, 1% Triton X-100, and 0.1% NP-40) for 25 min on ice. After the addition of 0.01 U/μl MNase (Sigma-Aldrich, St. Louis, MO) and 1 mM CaCl<sub>2</sub>, the mixtures were incubated for 5 min at 37°C. After 1 mM EGTA was added, the mixtures were centrifuged at 16,100 g for 15 min at 4°C. The resultant supernatants were collected as chromatin-bound protein fractions.

#### *Western blotting*

The extracted proteins were separated by SDS-PAGE and transferred to polyvinylidene difluoride membranes (BioRad, Hercules, CA). After blocking with 5% non-fat dry milk or bovine serum albumin, the membranes were incubated overnight at 4°C with the indicated antibodies (Supplementary Table S1). Following incubation with an appropriate secondary antibody, bound antibodies were detected with an ECL (Thermo Scientific Pierce Protein Biology Products, Rockford, IL) or ECL prime Western blotting detection system (GE Healthcare). For detection of the phosphorylated form of HP1γ, 100 μM of acrylamide-pendant phos-tag ligand (Wako, Osaka, Japan) and 0.1 mM of MnCl<sub>2</sub> were added to the separating gel before polymerization. Phosphorylation of HP1γ was detected as shifted bands using an anti-HP1γ antibody or anti-HA antibody.

#### *Immunoprecipitation*

HCT116 cells were transfected with the indicated plasmids for 24 or 48 h, and nuclear extracts were prepared as described above, mixed with an anti-HA antibody, anti-FLAG, or anti-histone H3K9me3, and rotated overnight at 4°C. After protein-A/G-agarose beads (Exalpha, Boston, MA) were added, the mixtures were further rotated for 2 h at 4°C. Immunoprecipitated proteins were collected by centrifugation, washed with PBS, and

analyzed by Western blotting.

#### *LC-MS/MS analysis of HIPK2-associating proteins*

For LC-MS/MS analysis of HIPK2-associating proteins, HCT116 cells were transfected with the FLAG-HIPK2-encoding vector or an empty vector for 48 h. Nuclear fractions were extracted, mixed with EZview red anti-FLAG M2 affinity gels (Sigma-Aldrich), and rotated overnight at 4°C. The beads were washed with Tris-buffered saline (TBS), and immunoprecipitated proteins were eluted by incubation in TBS containing 1 mg/ml 3 x FLAG peptide (Sigma-Aldrich) for 30 min on ice. The eluted proteins were separated by SDS-PAGE, visualized with a silver staining kit (Wako), and subjected to LC-MS/MS analysis. Data were analyzed with Mascot Search (Matrix Science, Boston, MA) and Scaffold software (Proteome Software, Inc., Portland, OR). MASCOT scores > 38 indicate identity or extensive homology ( $P < 0.05$ ).

#### *Immunofluorescence*

Cells growing on glass bottom dishes (MatTek Corporation, Ashland, MA) were rinsed in PBS and fixed in 3% (w/v) paraformaldehyde in phosphate buffer at room temperature. Fixed cells were permeabilized in 0.1% Triton X-100. After blocking with 4% Block-Ace (DS Pharma Biomedical, Osaka, Japan) at room temperature, cells were incubated overnight with anti-phospho-histone H2A.X (Ser139) (Supplementary Table S1) at 4°C. After washing, cells were treated with Alexa Fluor 488-conjugated anti-mouse IgG (Invitrogen). Nuclei were stained with TO-PRO-3 (Molecular Probes, Eugene, OR). The specimens were mounted in Vectashield mounting medium (Vector Laboratories, Burlingame, CA) and examined by confocal laser-scanning microscopy (FluoView FV1000; Olympus, Tokyo, Japan).

*In vitro kinase assay*

*Escherichia coli* DH5 $\alpha$  were transformed with pGEX6p-1-HP1 $\gamma$ . To express GST-HP1 $\gamma$  proteins, the transformed DH5 $\alpha$  bacterial cells were incubated with 1 mM isopropyl  $\beta$ -D-1-thiogalactopyranoside for 3 h at 20°C. The bacteria were centrifuged, lysed with 1% TritonX-100 in PBS, and sonicated. After centrifugation, the supernatants were incubated with glutathione sepharose 4B beads (GE Healthcare) for 1 h at 4°C. Beads were washed with 1% TritonX-100 in PBS and then with PreScission protease buffer (20 mM HEPES-NaOH, pH7.4, containing 150 mM NaCl, 1 mM EDTA, and 2 mM dithiothreitol). They were then incubated with PreScission protease buffer containing 15 U of PreScission protease (GE Healthcare) overnight at 4°C. The recombinant HP1 $\gamma$  protein (10  $\mu$ g) was incubated with 5  $\mu$ Ci  $\gamma$ <sup>32</sup>P-ATP and 20  $\mu$ M ATP in the presence of immunoprecipitated FLAG-HIPK2 or FLAG-HIPK2-KD in 25 mM HEPES-NaOH, pH7.4, containing 10 mM MgCl<sub>2</sub>, 2 mM dithiothreitol for 20 min at 22°C. The reaction was terminated by boiling for 5 min after adding SDS-Laemmli buffer. After separation by SDS-PAGE, gels were fixed, dried, and quantified using an FLA9000 system (GE Healthcare).

## **CONFLICT OF INTEREST**

The authors declare no conflict of interest.

## **ACKNOWLEDGEMENTS**

This work was supported by JSPS KAKENHI Grant Number 24-8354 (to YA).



**REFERENCES**

- 1 Soria G, Polo SE, Almouzni G. Prime, repair, restore: the active role of chromatin in the DNA damage response. *Mol Cell* 2012; **46**: 722-734.
- 2 Sombroek D, Hofmann TG. How cells switch HIPK2 on and off. *Cell Death Differ* 2009; **16**: 187-194.
- 3 Puca R, Nardinocchi L, Givol D, D'Orazi G. Regulation of p53 activity by HIPK2: molecular mechanisms and therapeutical implications in human cancer cells. *Oncogene* 2010; **29**: 4378-4387.
- 4 Winter M, Sombroek D, Dauth I, Moehlenbrink J, Scheuermann K, Crone J *et al.*, Control of HIPK2 stability by ubiquitin ligase Siah-1 and checkpoint kinases ATM and ATR. *Nat Cell Biol* 2008; **10**: 812-824.
- 5 Gresko E, Roscic A, Ritterhoff S, Vichalkovski A, del Sal G, Schmitz ML. Autoregulatory control of the p53 response by caspase-mediated processing of HIPK2. *EMBO J* 2006; **25**: 1883-1894.
- 6 Saul VV, de la Vega L, Milanovic M, Kruger M, Braun T, Fritz-Wolf K *et al.* HIPK2 kinase activity depends on cis-autophosphorylation of its activation loop. *J Mol Cell Biol* 2013; **5**: 27-38.
- 7 D'Orazi G, Cecchinelli B, Bruno T, Manni I, Higashimoto Y, Saito S *et al.* Homeodomain-interacting protein kinase-2 phosphorylates p53 at Ser46 and mediates apoptosis. *Nat Cell Biol* 2002; **4**: 11-19.
- 8 Hofmann TG, Moller A, Sirma H, Zentgraf H, Taya Y, Droge W *et al.* Regulation of p53 activity by its interaction with homeodomain-interacting protein kinase-2. *Nat Cell Biol* 2002; **4**: 1-10.
- 9 Hofmann TG, Glas C, Bitomsky N. HIPK2: A tumour suppressor that controls DNA damage-induced cell fate and cytokinesis. *Bioessays* 2013; **35**: 55-64.
- 10 Di Stefano V, Soddu S, Sacchi A, D'Orazi G. HIPK2 contributes to PCAF-mediated p53 acetylation and selective transactivation of p21Waf1 after nonapoptotic DNA damage. *Oncogene* 2005; **24**: 5431-5442.
- 11 Papamichos-Chronakis M, Peterson CL. Chromatin and the genome integrity network. *Nat Rev Genet* 2013; **14**: 62-75.
- 12 Price BD, D'Andrea AD. Chromatin remodeling at DNA double-strand breaks. *Cell* 2013; **152**:1344-1354.
- 13 Kwon SH, Workman JL. The heterochromatin protein 1 (HP1) family: put away a bias toward HP1. *Mol Cells* 2008; **26**: 217-227.
- 14 Lomberk G, Wallrath L, Urrutia R. The heterochromatin protein 1 family. *Genome Biol* 2006; **7**: 228.
- 15 Nielsen AL, Oulad-Abdelghani M, Ortiz JA, Remboutsika E, Chambon P, Losson R. Heterochromatin formation in mammalian cells: interaction between histones and HP1 proteins *Mol Cell* 2001; **7**: 729-739.
- 16 Kwon SH, Workman JL. The changing faces of HP1: From heterochromatin formation and gene silencing to euchromatic gene expression: HP1 acts as a positive regulator of transcription. *Bioessays* 2011; **33**: 280-289.

- 17 Ayoub N, Jeyasekharan AD, Bernal JA, Venkitaraman AR. HP1-beta mobilization promotes chromatin changes that initiate the DNA damage response. *Nature* 2008; **453**: 682-686.
- 18 Lee YH, Kuo CY, Stark JM, Shih HM, Ann DK. HP1 promotes tumor suppressor BRCA1 functions during the DNA damage response. *Nucleic Acids Res* 2013; **41**: 5784-5798.
- 19 Luijsterburg MS, Dinant C, Lans H, Stap J, Wiernasz E, Lagerwerf S *et al*. Heterochromatin protein 1 is recruited to various types of DNA damage. *J Cell Biol* 2009; **185**: 577-586.
- 20 Zarebski M, Wiernasz E, Dobrucki JW. Recruitment of heterochromatin protein 1 to DNA repair sites. *Cytometry A* 2009; **75**: 619-625.
- 21 Kurokawa K, Akaike Y, Masuda K, Kuwano Y, Nishida K, Yamagishi N *et al*. Downregulation of serine/arginine-rich splicing factor 3 induces G1 cell cycle arrest and apoptosis in colon cancer cells. *Oncogene* 2014; **33**: 1407-1417.
- 22 Hailemariam K, Iwasaki K, Huang BW, Sakamoto K, Tsuji Y. Transcriptional regulation of ferritin and antioxidant genes by HIPK2 under genotoxic stress. *J Cell Sci* 2010; **123**: 3863-3871.
- 23 Rastogi RP, Richa, Kumar A, Tyagi MB, Sinha RP. Molecular mechanisms of ultraviolet radiation-induced DNA damage and repair. *J Nucleic Acids* 2010; **2010**: 592980.
- 24 Lee DH, Chowdhury D. What goes on must come off: phosphatases gate-crash the DNA damage response. *Trends Biochem Sci* 2011; **36**: 569-577.
- 25 Mah LJ, El-Osta A, Karagiannis TC. gammaH2AX: a sensitive molecular marker of DNA damage and repair. *Leukemia* 2010; **24**: 679-686.
- 26 Lobrich M, Shibata A, Beucher A, Fisher A, Ensminger M, Goodarzi AA *et al*. gammaH2AX foci analysis for monitoring DNA double-strand break repair: strengths, limitations and optimization. *Cell Cycle* 2010; **9**: 662-669.
- 27 Kim YH, Choi CY, Lee SJ, Conti MA, Kim Y. Homeodomain-interacting protein kinases, a novel family of co-repressors for homeodomain transcription factors. *J Biol Chem* 1998; **273**: 25875-25879.
- 28 Isono K, Nemoto K, Li Y, Takada Y, Suzuki R, Katsuki M *et al*. Overlapping roles for homeodomain-interacting protein kinases hipk1 and hipk2 in the mediation of cell growth in response to morphogenetic and genotoxic signals. *Mol Cell Biol* 2006; **26**: 2758-2771.
- 29 Rinaldo C, Prodosmo A, Siepi F, Soddu S. HIPK2: a multitalented partner for transcription factors in DNA damage response and development. *Biochem Cell Biol* 2007; **85**: 411-418.
- 30 Smothers JF, Henikoff S. The HP1 chromo shadow domain binds a consensus peptide pentamer. *Curr Biol* 2000; **10**: 27-30.
- 31 LeRoy G, Weston JT, Zee BM, Young NL, Plazas-Mayorca MD, Garcia BA. Heterochromatin protein 1 is extensively decorated with histone code-like post-translational modifications. *Mol Cell Proteomics* 2009; **8**: 2432-2442.
- 32 Yamada D, Perez-Torrado R, Filion G, Caly M, Jammart B, Devignot V *et al*. The human protein kinase HIPK2 phosphorylates and downregulates the methyl-binding transcription factor ZBTB4. *Oncogene* 2009; **28**: 2535-2544.
- 33 Wei G, Ku S, Ma GK, Saito S, Tang AA, Zhang J *et al*. HIPK2 represses beta-catenin-mediated transcription, epidermal stem cell expansion, and skin

- tumorigenesis. *Proc Natl Acad Sci U S A* 2007; **104**: 13040-13045.
- 34 Rinaldo C, Moncada A, Gradi A, Ciuffini L, D'Eliseo D, Siepi F *et al*. HIPK2 controls cytokinesis and prevents tetraploidization by phosphorylating histone H2B at the midbody. *Mol Cell* 2012; **47**: 87-98.
- 35 Lomberk G, Bensi D, Fernandez-Zapico ME, Urrutia R. Evidence for the existence of an HP1-mediated subcode within the histone code. *Nat Cell Biol* 2006; **8**: 407-415.
- 36 Grzenda A, Leonard P, Seo S, Mathison AJ, Urrutia G, Calvo E *et al*. Functional impact of Aurora A-mediated phosphorylation of HP1 $\gamma$  at serine 83 during cell cycle progression. *Epigenetics Chromatin* 2013; **6**: 21.
- 37 Zhang Q, Yoshimatsu Y, Hildebrand J, Frisch SM, Goodman RH. Homeodomain interacting protein kinase 2 promotes apoptosis by downregulating the transcriptional corepressor CtBP. *Cell* 2003; **115**: 177-186.
- 38 Nardinocchi L, Puca R, Sacchi A, D'Orazi G. HIPK2 knock-down compromises tumor cell efficiency to repair damaged DNA. *Biochem Biophys Res Commun* 2007; **361**: 249-255.
- 39 Pontarin G, Ferraro P, Bee L, Reichard P, Bianchi V. Mammalian ribonucleotide reductase subunit p53R2 is required for mitochondrial DNA replication and DNA repair in quiescent cells. *Proc Natl Acad Sci U S A* 2012; **109**: 13302-13307.
- 40 Yamaguchi T, Matsuda K, Sagiya Y, Iwadate M, Fujino MA, Nakamura Y *et al*. p53R2-dependent pathway for DNA synthesis in a p53-regulated cell cycle checkpoint. *Cancer Res* 2001; **61**: 8256-8262.
- 41 Choi DW, Na W, Kabir MH, Yi E, Kwon S, Yeom J *et al*. WIP1, a homeostatic regulator of the DNA damage response, is targeted by HIPK2 for phosphorylation and degradation. *Mol Cell* 2013; **51**: 374-385.
- 42 Baldeyron C, Soria G, Roche D, Cook AJ, Almouzni G. HP1 $\alpha$  recruitment to DNA damage by p150CAF-1 promotes homologous recombination repair. *J Cell Biol* 2011; **193**: 81-95.
- 43 Dinant C, Luijsterburg MS. The emerging role of HP1 in the DNA damage response. *Mol Cell Biol* 2009; **29**: 6335-6340.
- 44 Minc E, Courvalin JC, Buendia B. HP1 $\gamma$  associates with euchromatin and heterochromatin in mammalian nuclei and chromosomes. *Cytogenet Cell Genet* 2000; **90**: 279-284.
- 45 Goodarzi AA, Noon AT, Deckbar D, Ziv Y, Shiloh Y, Lobrich M *et al*. ATM signaling facilitates repair of DNA double-strand breaks associated with heterochromatin. *Mol Cell* 2008; **31**: 167-177.
- 46 Kim JA, Kruhlak M, Dotiwala F, Nussenzweig A, Haber JE. Heterochromatin is refractory to gamma-H2AX modification in yeast and mammals. *J Cell Biol* 2007; **178**: 209-218.
- 47 Noon AT, Shibata A, Rief N, Lobrich M, Stewart GS, Jeggo PA *et al*. 53BP1-dependent robust localized KAP-1 phosphorylation is essential for heterochromatic DNA double-strand break repair. *Nat Cell Biol* 2010; **12**: 177-184.
- 48 Chiolo I, Minoda A, Colmenares SU, Polyzos A, Costes SV, Karpen GH. Double-strand breaks in heterochromatin move outside of a dynamic HP1 $\alpha$  domain to complete recombinational repair. *Cell* 2011; **144**: 732-744.

- 49 Jakob B, Splinter J, Conrad S, Voss KO, Zink D, Durante M *et al*. DNA double-strand breaks in heterochromatin elicit fast repair protein recruitment, histone H2AX phosphorylation and relocation to euchromatin. *Nucleic Acids Res* 2011; **39**: 6489-6499.
- 50 Cann KL, Dellaire G. Heterochromatin and the DNA damage response: the need to relax. *Biochem Cell Biol* 2011; **89**: 45-60.
- 51 Hiragami-Hamada K, Shinmyozu K, Hamada D, Tatsu Y, Uegaki K, Fujiwara S *et al*. N-terminal phosphorylation of HP1 {alpha} promotes its chromatin binding. *Mol Cell Biol* 2011; **31**: 1186-1200.
- 52 Kuwano Y, Pullmann R Jr., Marasa BS, Abdelmohsen K, Lee EK, Yang X *et al*. NF90 selectively represses the translation of target mRNAs bearing an AU-rich signature motif. *Nucleic Acids Res* 2010; **38**: 225-238.
- 53 Mund A, Schubert T, Staeger H, Kinkley S, Reumann K, Kriegs M *et al*. SPOC1 modulates DNA repair by regulating key determinants of chromatin compaction and DNA damage response. *Nucleic Acids Res* 2012; **40**: 11363-11379.

Supplementary Information accompanies the paper on the *Oncogene* website  
(<http://www.nature.com/onc>).

**FIGURE LEGENDS**

**Figure 1.** Effects of HIPK2 knockdown on apoptosis after sublethal UV-C irradiation. **(a)** HCT116 cells were treated with 10 nM control, HIPK2#1, or HIPK2#2 siRNAs for 48 h and then exposed to 10 J/m<sup>2</sup> UV-C. After cultivation for the indicated times, apoptosis was analyzed using the DeadEnd Colorimetric TUNEL system. TUNEL-positive cells in each field were counted at least 10 fields for each sample, and data were expressed as percentages of apoptotic cells in three independent experiments. Bar, 100 μm. \*Significantly different by unpaired Student's *t*-test compared with control siRNA-treated cells ( $P < 0.01$ ). **(b)** Control or HIPK2 siRNA-treated cells were irradiated with 10 J/m<sup>2</sup> UV-C and cultured for 24 h. Levels of unprocessed or cleaved forms of caspase-9 and caspase-3 were measured by Western blotting using β-actin as a loading control. **(c)** After cells were treated with control or one of the HIPK2 siRNAs and then irradiated with 10 J/m<sup>2</sup> UV-C as in **(b)**, numbers of viable cells were counted. The data were normalized by numbers of untreated control cells and expressed as percentages in three independent experiments. \*Significantly different by unpaired Student's *t*-test compared with control siRNA-treated cells ( $P < 0.01$ ).

**Figure 2.** Effects of HIPK2 knockdown on UV-C-induced DNA damage. **(a)** HCT116 cells treated with control or HIPK2 siRNA#1 were irradiated with 10 J/m<sup>2</sup> UV-C and incubated for the indicated times. Genomic DNA was purified and used for the determination of 6-4PP contents using ELISA. Each point represents the mean ± SD from three independent experiments. \*Significantly different by unpaired Student's *t*-test ( $P < 0.05$ ). **(b)** HCT116 cells were treated as in **(a)**. Amounts of γH2A.X were measured by Western blotting using β-actin as a loading control. γH2A.X signals were quantified by densitometry. Time-dependent changes in γH2A.X levels are expressed as fold changes (γH2A.X/β-actin) in three independent experiments. **(c)** Wild-type or *hipk1*<sup>-/-</sup>*hipk2*<sup>-/-</sup> MEFs were irradiated with 5 J/m<sup>2</sup>

UV-C and incubated for the indicated times. These cells were then stained with an anti- $\gamma$ H2A.X antibody (green), and nuclei were stained with TO-PRO-3 (blue). Bar, 100  $\mu$ m. Percentages of  $\gamma$ H2A.X-positive cells (> 10  $\gamma$ H2A.X foci in a cell) in 10 different fields were calculated. Values are means  $\pm$  SD from three independent experiments. \*Significantly different by unpaired Student's *t*-test ( $P < 0.01$ ).

**Figure 3.** Association between HIPK2 and HP1 $\gamma$ . **(a)** Nuclear proteins were extracted from HCT116 cells transfected with the FLAG-HIPK2-encoding vector or an empty vector for 48 h. After immunoprecipitation with an anti-FLAG antibody, the purified proteins were resolved by SDS-PAGE and visualized by silver staining. The indicated protein band with a molecular mass of 22 kDa was analyzed by LC-MS/MS. **(b)** HCT116 cells were transfected with the FLAG-HIPK2-encoding vector or an empty vector for 48 h. Amounts of FLAG-HIPK2, HP1 $\alpha$ , HP1 $\beta$ , and HP1 $\gamma$  in nuclear extracts (input) and in immunoprecipitates (using an anti-FLAG antibody [FLAG-IP]) were measured by Western blotting using  $\beta$ -actin as a loading control. **(c)** HCT116 cells were co-transfected with the FLAG-HIPK2-encoding vector and the vector encoding HA-HP1 $\alpha$ , HA-HP1 $\beta$ , or HA-HP1 $\gamma$  for 48 h. Amounts of FLAG-HIPK2 and HA-tagged HP1 proteins in nuclear proteins (input) and immunoprecipitates (using an anti-HA antibody [HA-IP]) were measured by Western blotting. **(d)** p53<sup>-/-</sup> HCT116 cells were co-transfected with the vectors encoding HA-HP1 $\gamma$  and FLAG-HIPK2 or an empty vector for 48 h. Amounts of FLAG-HIPK2 and HA-HP1 $\gamma$  in nuclear proteins (input) and immunoprecipitates (HA-IP) were measured by Western blotting. **(e)** HEK293T cells were treated as in **(b)**. Amounts of FLAG-HIPK2 and HP1 $\gamma$  in nuclear proteins (input) and immunoprecipitates (FLAG-IP) were measured by Western blotting. **(f)** The scheme of the consensus HP1-binding motifs (525-PFVTM-529 and 883-PTVSV-887) within HIPK2. The critical residues (V527 and V885) were mutated into alanine within

HIPK2mt1 and HIPK2mt2, respectively. HCT116 cells were co-transfected with the HA-HP1 $\gamma$ -encoding vector and the vector encoding FLAG-HIPK2, FLAG-HIPK2mt1, or FLAG-HIPK2mt2 for 48 h. Amounts of FLAG-HIPK2 and HA-HP1 $\gamma$  in nuclear proteins (input) and immunoprecipitates with an anti-FLAG (FLAG-IP) or an anti-HA antibody (HA-IP) were measured by Western blotting.

**Figure 4.** Phosphorylation of HP1 $\gamma$  by HIPK2. **(a)** HCT116 cells were transfected with the vector encoding FLAG-HIPK2 or FLAG-HIPK2-KD, or an empty vector for 48 h. Nuclear proteins prepared from these cells were immunoprecipitated using an anti-FLAG antibody and incubated with  $\gamma^{32}\text{P}$ -ATP, unlabeled ATP, and recombinant HP1 $\gamma$ . They were separated by SDS-PAGE and visualized by autoradiography. Amounts of FLAG-HIPK2, FLAG-HIPK2-KD, and recombinant HP1 $\gamma$  were confirmed to be appropriate using Western blotting. **(b)** After HCT116 cells were treated with a siRNA targeting HIPK2 3'UTR (HIPK2 3'U siRNA) for 24 h, they were transfected with the vector encoding either FLAG-HIPK2 or FLAG-HIPK2-KD, or an empty vector and then irradiated with 10 J/m<sup>2</sup> UV-C. After cultivation for 12 h, phosphorylation of HP1 $\gamma$  (phospho-HP1 $\gamma$ ) in these cells was detected by phos-tag SDS-PAGE using an anti-HP1 $\gamma$  antibody. Amounts of HP1 $\gamma$ , FLAG-HIPK2, and  $\beta$ -actin were measured by Western blotting. **(c)** Levels of phospho-HP1 $\gamma$  and  $\beta$ -actin in **(b)** were quantified by densitometry, and time-dependent changes in phospho-HP1 $\gamma$  levels are expressed as fold changes (phospho-HP1 $\gamma$ / $\beta$ -actin). Values are the means  $\pm$  SD from three independent experiments. \*Significantly different by unpaired Student's *t*-test ( $P < 0.05$ ). **(d)** After HCT116 cells were treated with control or HIPK2 3'U siRNA for 24 h, they were transfected with the vector encoding either FLAG-HIPK2 or FLAG-HIPK2-KD, or an empty vector for 24 h and then irradiated with 10 J/m<sup>2</sup> UV-C. After incubation for 24 h, amounts of  $\gamma\text{H2A.X}$ , FLAG-HIPK2, FLAG-HIPK2-KD and  $\beta$ -actin were measured by Western blotting.



Changes in  $\gamma$ H2A.X levels are expressed as fold changes ( $\gamma$ H2A.X/ $\beta$ -actin). Each value represents the mean  $\pm$  SD from three independent experiments. \*Significantly different by unpaired Student's *t*-test ( $P < 0.05$ ).

**Figure 5.** Effect of HP1 $\gamma$  knockdown on UV-C-induced apoptosis. **(a)** HCT116 cells were treated with 10 nM control or HP1 $\gamma$  siRNA for 48 h, and *HPI1 $\gamma$*  mRNA levels were measured by qPCR using *GAPDH* mRNA as an endogenous quantitative control. Values are the means  $\pm$  SD from three independent experiments. \*Significantly different by unpaired Student's *t*-test ( $P < 0.01$ ). HP1 $\gamma$  protein levels measured by Western blotting are shown in the lower panel. **(b)** Control or HP1 $\gamma$  siRNA-treated HCT116 cells were irradiated with 10 J/m<sup>2</sup> UV-C for the indicated times. Amounts of  $\gamma$ H2A.X and HP1 $\gamma$  were measured by Western blotting. **(c)** Control or HP1 $\gamma$  siRNA-treated HCT116 cells were irradiated with 10 J/m<sup>2</sup> UV-C and incubated for the indicated times. Levels of unprocessed or cleaved forms of caspase-3 and HP1 $\gamma$  were measured by Western blotting.

**Figure 6.** HIPK2-dependent regulation of HP1 $\gamma$  binding to histone H3K9me3. **(a)** Endogenous HIPK2 in HCT116 cells was silenced with HIPK2 3'UTR-targeting siRNA. After these cells were treated with an empty vector (mock) or co-transfected with the HA-HP1 $\gamma$ -encoding vector and the vector encoding FLAG-HIPK2 (WT), FLAG- HIPK2mt2 (mt2), or FLAG-HIPK2 KD (KD) for 48 h. After these cells were left untreated or exposed to 10 J/m<sup>2</sup> UV-C and incubated for 12 h, amounts of HA-HP1 $\gamma$ , histone H3, FLAG-HIPK2, and  $\beta$ -actin in cell lysates (input) prepared from these cells were measured by Western blotting. The cell lysates were immunoprecipitated with an anti-histone H3K9me3. Amounts of HA-HP1 $\gamma$  and histone H3K9me3 in the immunoprecipitates were measured by Western

blotting using anti-HA and anti-histone H3K9me3 antibodies, respectively. Levels of HA-HP1 $\gamma$  in immunoprecipitates and input were quantified by densitometry. Relative intensity of HA-HP1 $\gamma$  (histone H3K9me3-IP/input) was calculated and normalized for that measured in mock-transfected, untreated cells. Values are the means  $\pm$  SD in three independent experiments. \*Significantly different before and after UV-C exposure by unpaired Student's *t*-test ( $P < 0.05$ ). **(b)** FLAG-HIPK2 (WT), FLAG- HIPK2mt2 (mt2), or FLAG-HIPK2 KD (KD) was overexpressed in the HIPK2 knockdown cells with HIPK2 3'UTR-targeting siRNA. Soluble and chromatin-bound protein fractions were prepared before and after exposure to 10 J/m<sup>2</sup> UV-C. Amounts of HP1 $\gamma$ , HP1 $\alpha$ , HP1 $\beta$ , histone H3, and  $\beta$ -actin were measured by Western blotting. Levels of HP1 $\gamma$  and  $\beta$ -actin in each fraction were quantified by densitometry. Relative intensity (HP1 $\gamma$ / $\beta$ -actin) was normalized for that measured in mock-transfected, untreated cells. Values are the means  $\pm$  SD in three independent experiments. \*Significantly different before and after UV-C exposure by unpaired Student's *t*-test ( $P < 0.05$ ).

Figure 1. Akaike et al.

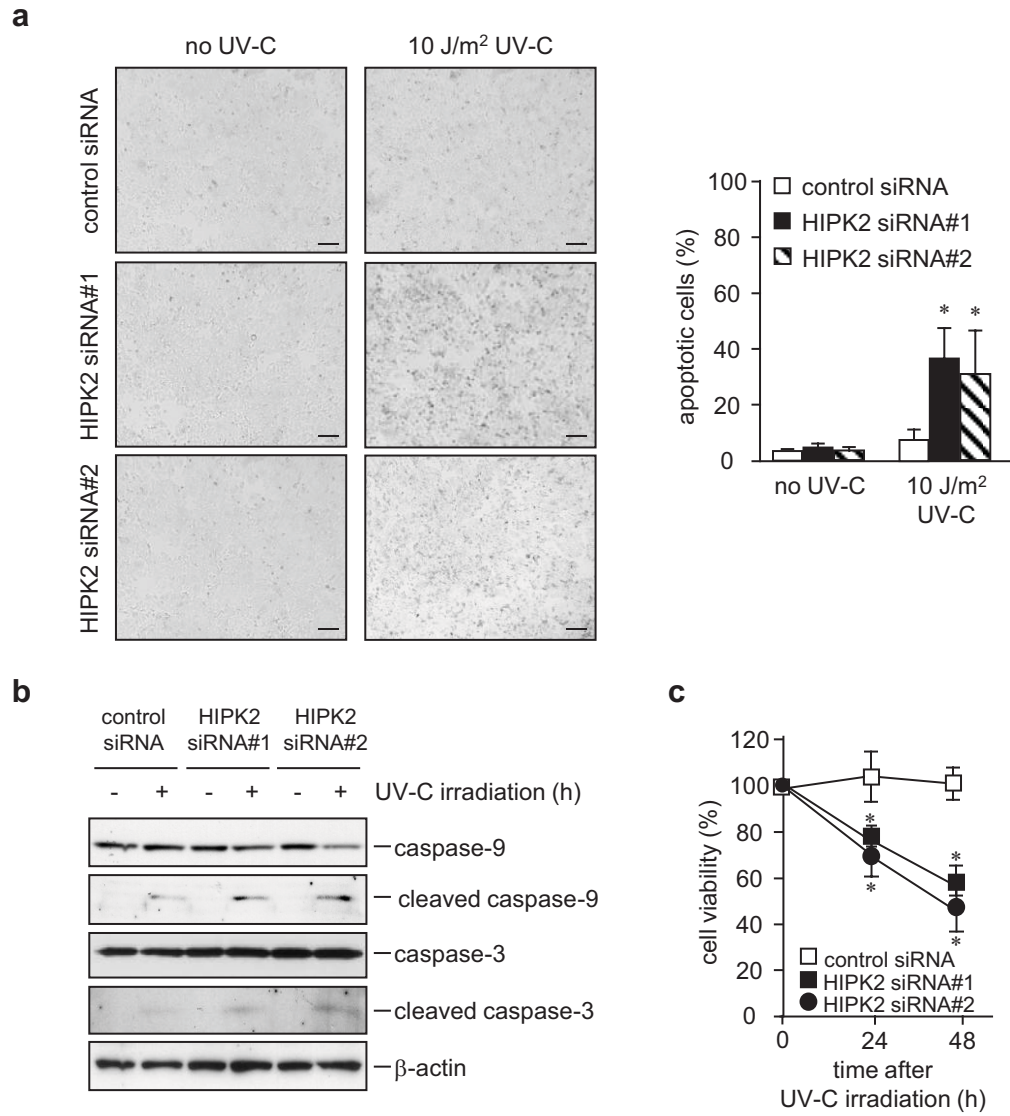


Figure 2. Akaike et al.

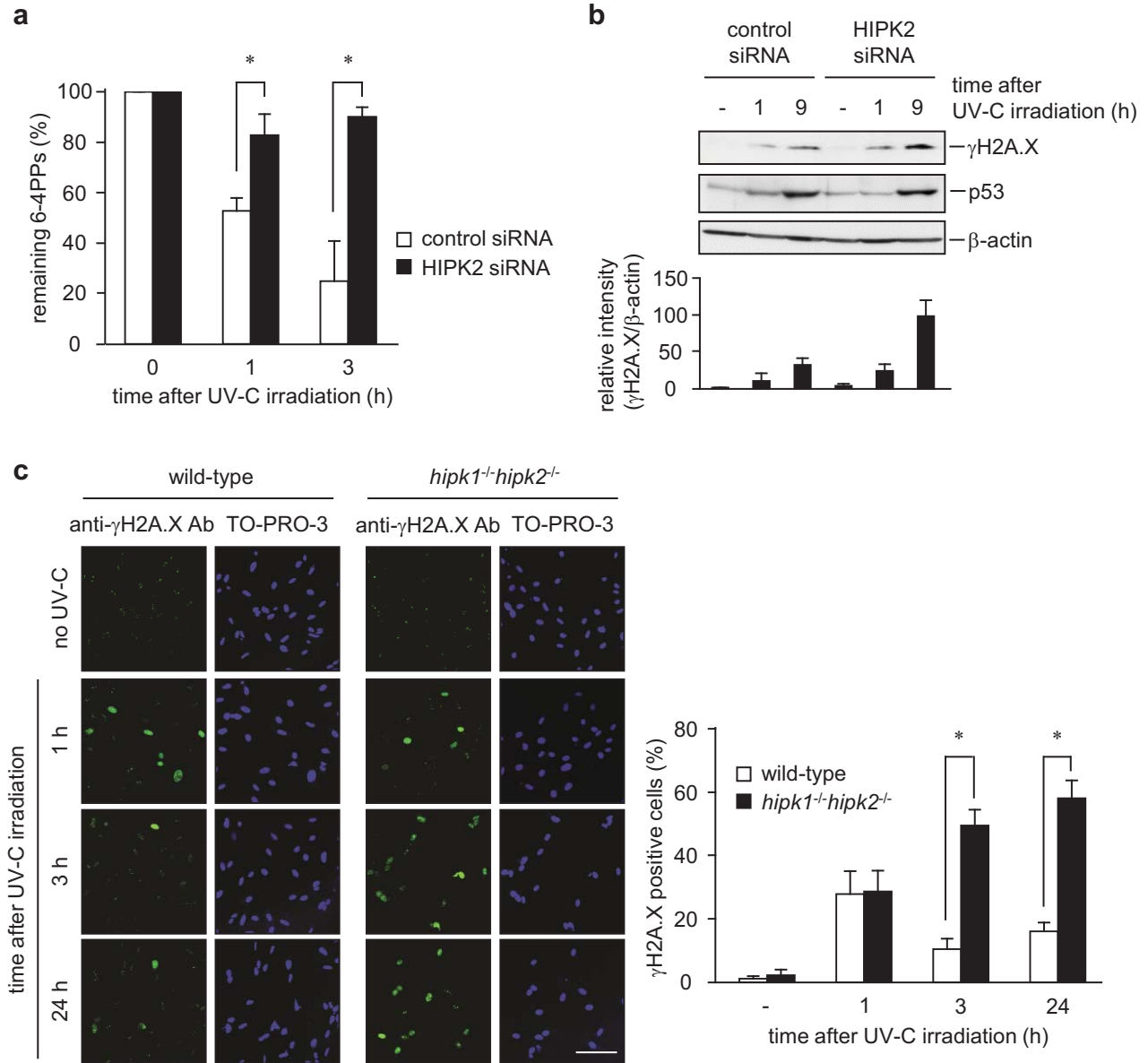


Figure 3. Akaike et al.

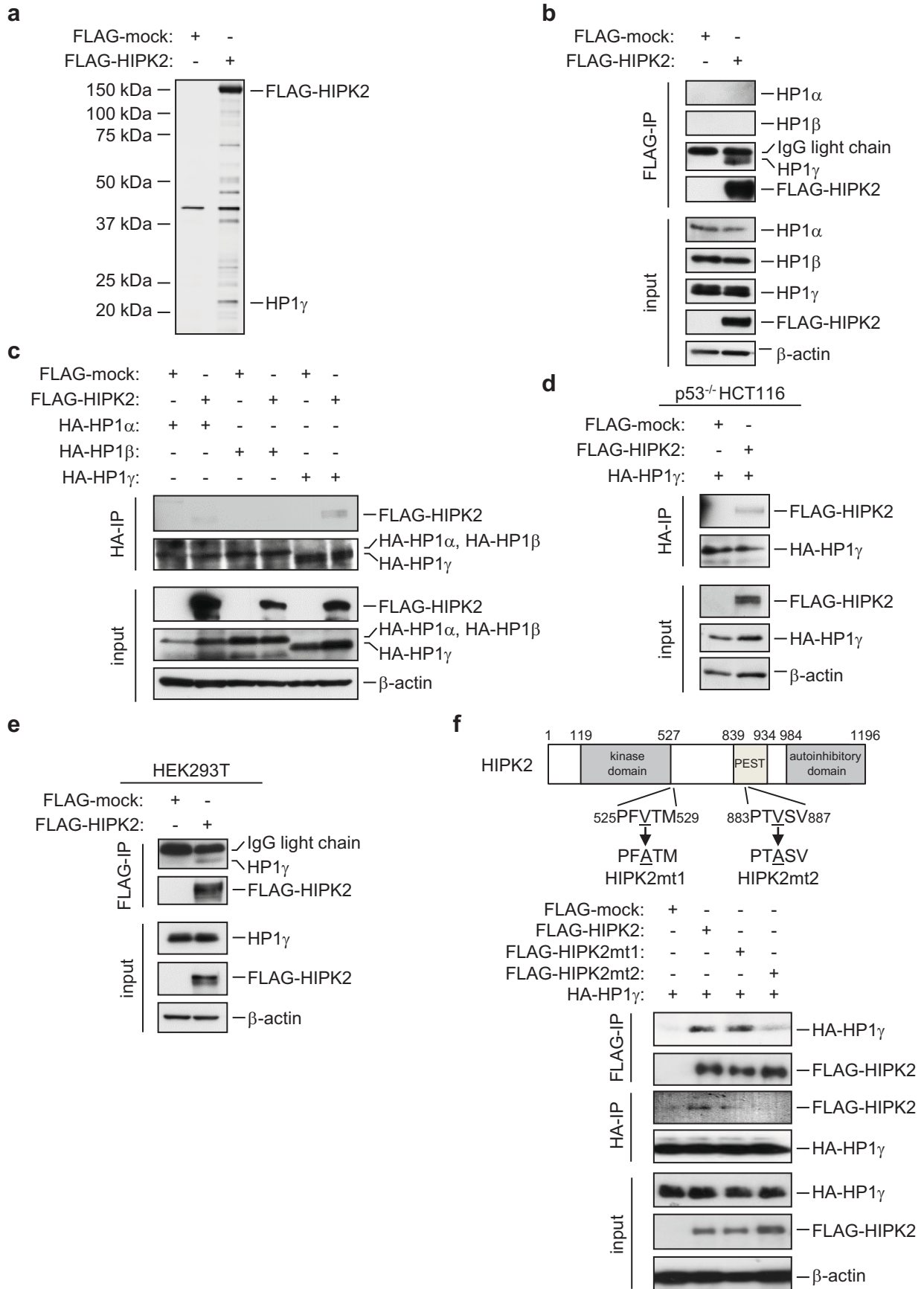


Figure 4. Akaike et al.

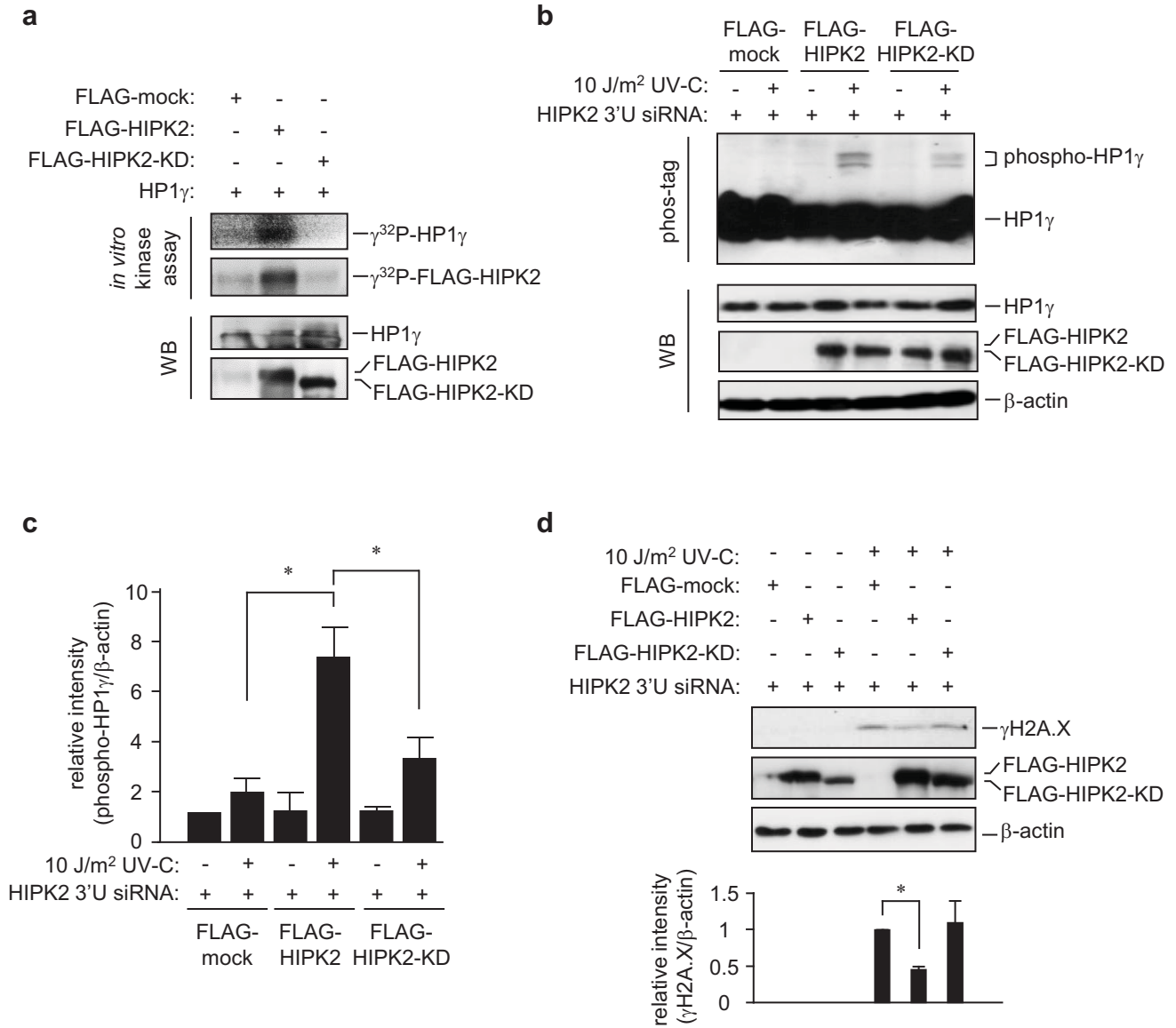


Figure 5. Akaike et al.

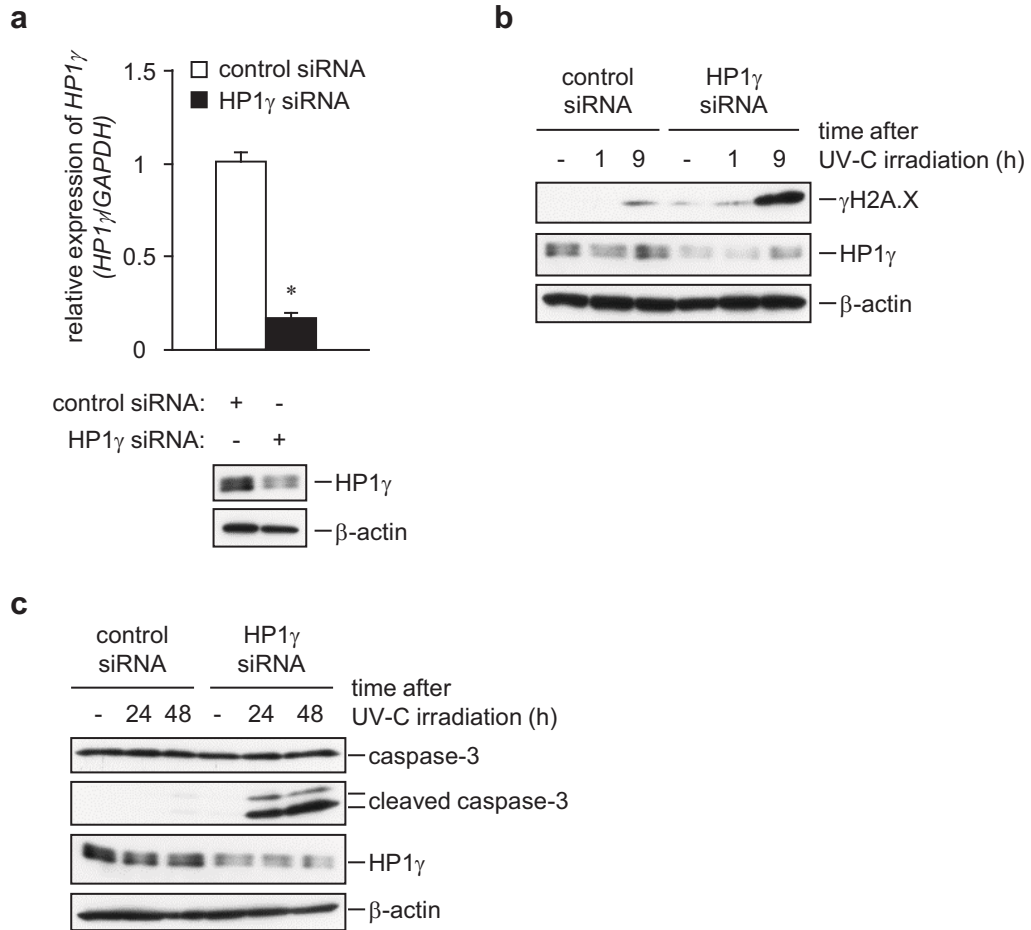
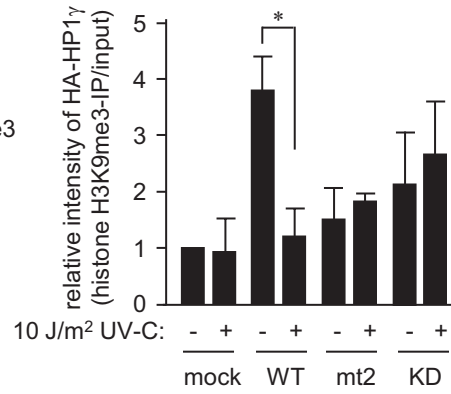
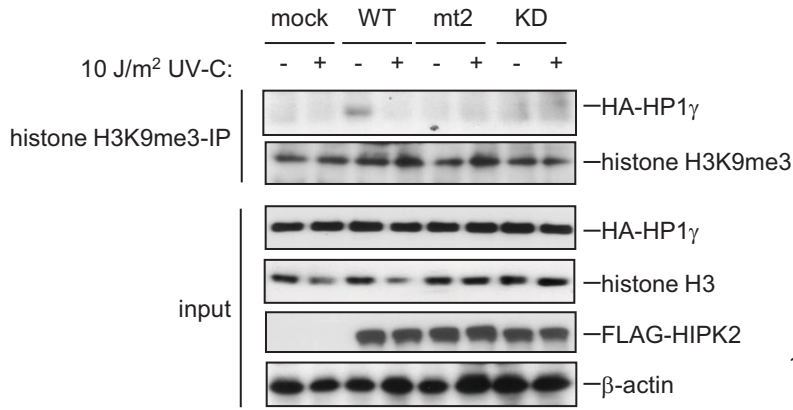
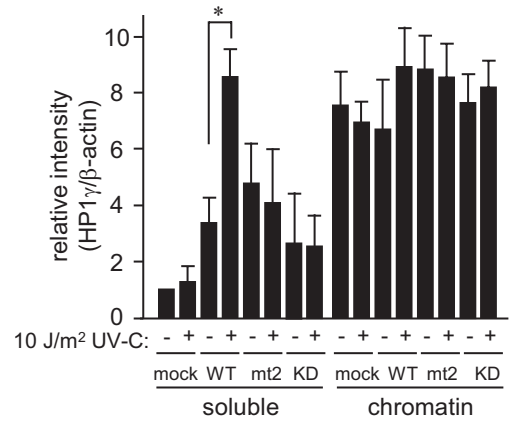
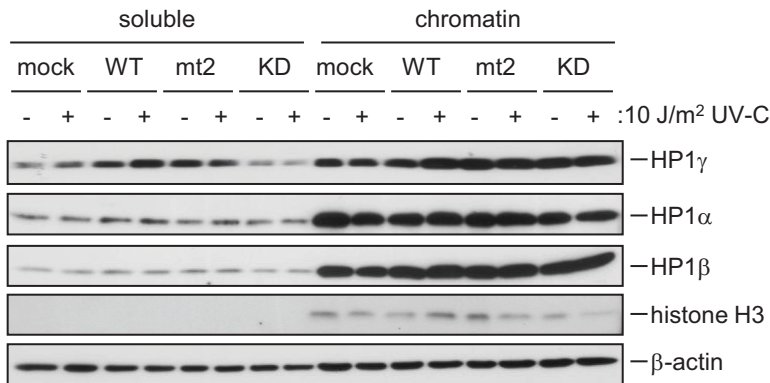


Figure 6. Akaike et al.

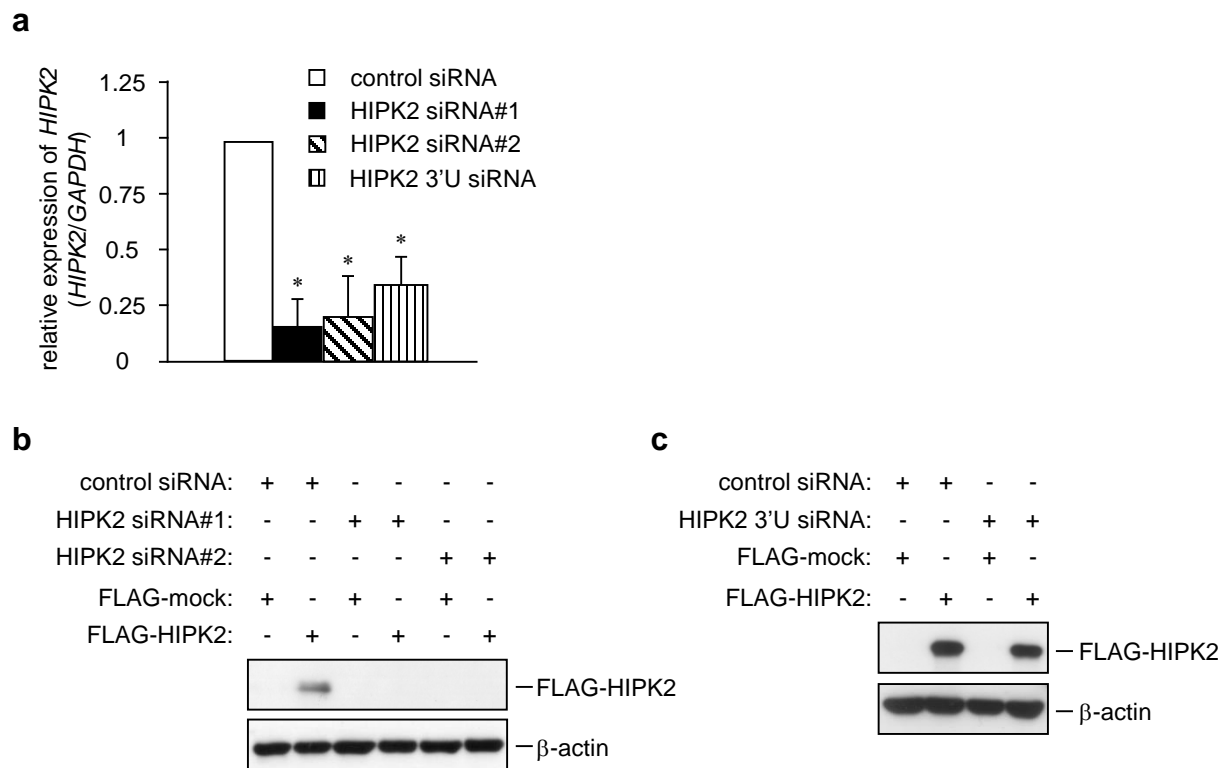
**a**



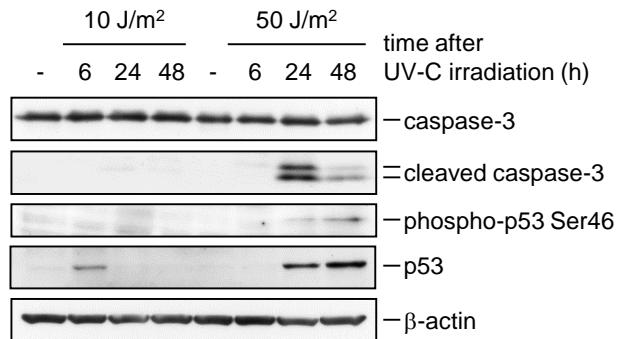
**b**



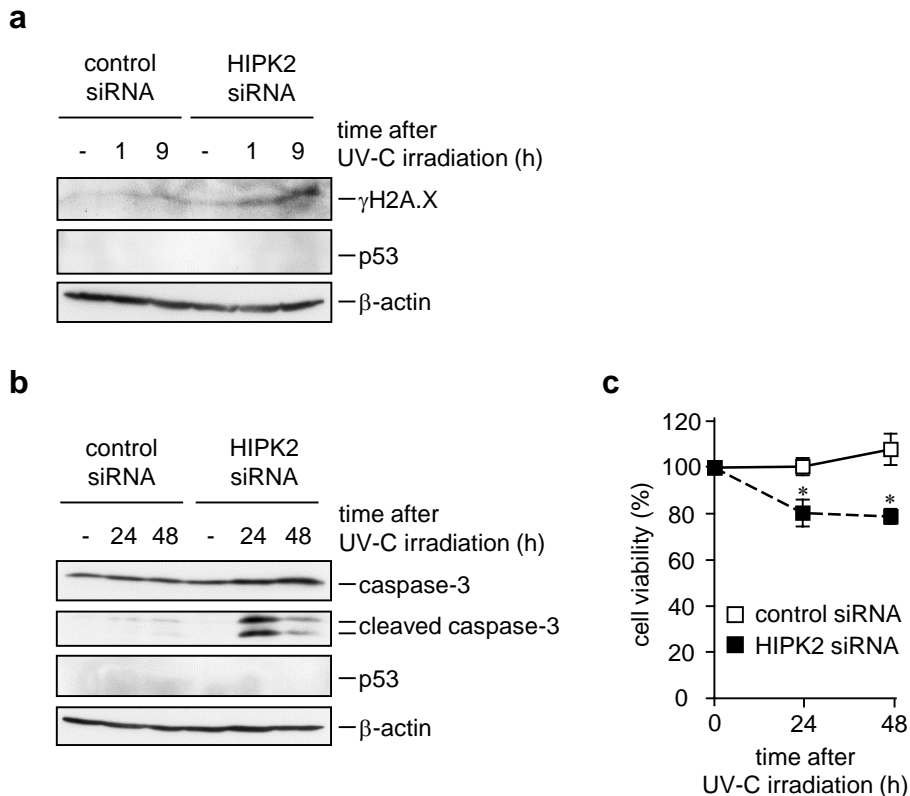




**Supplementary Figure S1.** The knockdown efficiency of *HIPK2* siRNAs. **(a)** HCT116 cells were treated with control or *HIPK2* siRNAs (*HIPK2* siRNA#1, #2 or *HIPK2* 3' UTR (*HIPK2* 3'U siRNA) for 48 h, and *HIPK2* mRNA levels were measured by qPCR using *GAPDH* mRNA as an endogenous quantitative control. Values are the means  $\pm$  SD from three independent experiments. \*Significantly different by unpaired Student's *t*-test ( $P < 0.01$ ). **(b)** HCT116 cells were co-transfected with control, *HIPK2* siRNA#1 or #2 and the FLAG-*HIPK2*-encoding vector or an empty vector for 48 h. Amounts of FLAG-*HIPK2* were measured by Western blotting using  $\beta$ -actin as a loading control. **(c)** HCT116 cells were co-transfected with control or *HIPK2* 3' U siRNA and the FLAG-*HIPK2*-encoding vector or an empty vector for 48 h. Amounts of FLAG-*HIPK2* were measured by Western blotting using  $\beta$ -actin as a loading control.

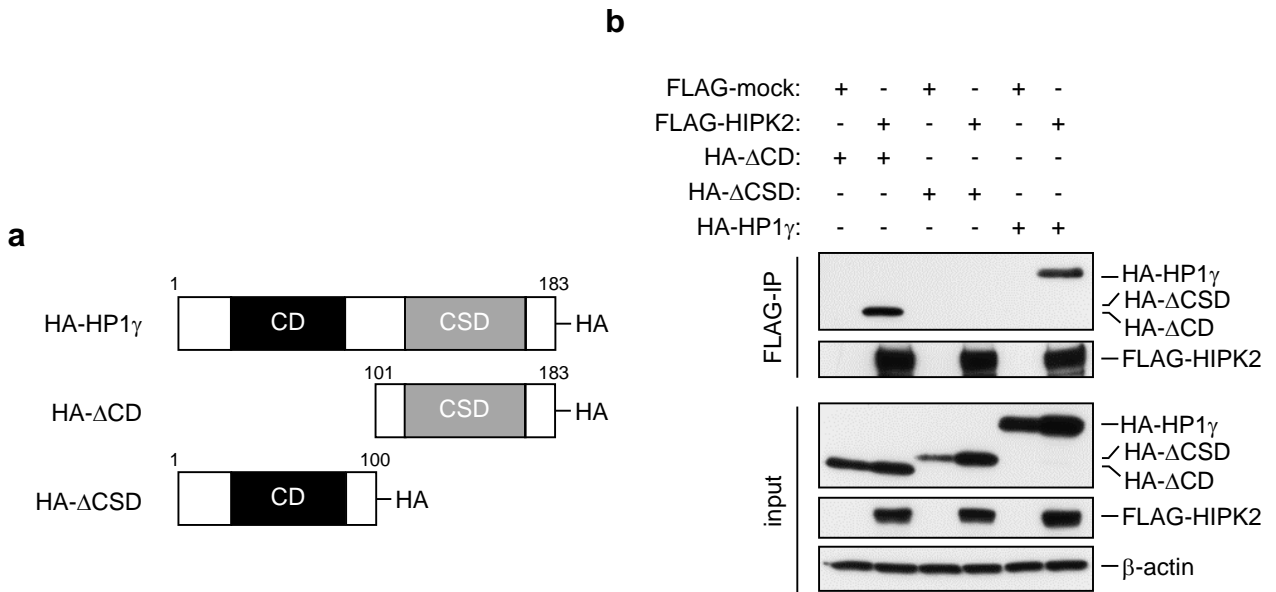


**Supplementary Figure S2.** Effects of sublethal (10 J/m<sup>2</sup>) and lethal (50 J/m<sup>2</sup>) UV-C irradiation on HCT116 cells. HCT116 cells were irradiated with 10 or 50 J/m<sup>2</sup> UV-C and incubated for the indicated times. Levels of unprocessed or cleaved forms of caspase-3, phosphorylated p53 at Ser46 (phospho-p53 Ser46), and p53 were measured by Western blotting using β-actin as a loading control.

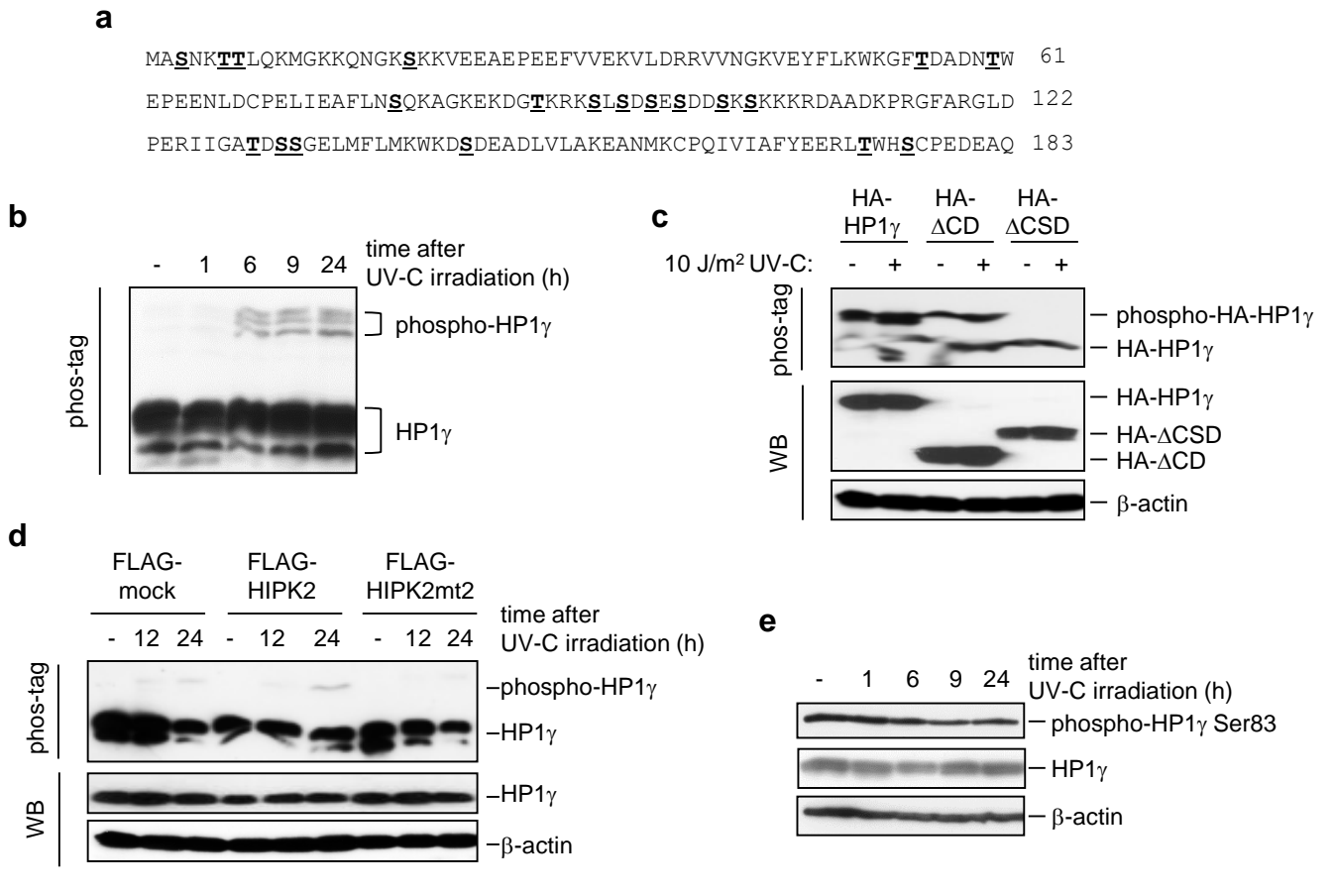


**Supplementary Figure S3.** Effects of HIPK2 knockdown in p53-null ( $p53^{-/-}$ ) HCT116 cells. **(a)** After  $p53^{-/-}$  HCT116 cells (kindly provided by Dr. Vogelstein) were treated with control siRNA or HIPK2 siRNA#1, they were irradiated with  $10 \text{ J/m}^2$  UV-C and incubated for the indicated times. Amounts of  $\gamma$ H2A.X and p53 were measured by Western blotting using  $\beta$ -actin as a loading control. **(b)** Control siRNA or HIPK2 siRNA#1-treated  $p53^{-/-}$  HCT116 cells were irradiated with  $10 \text{ J/m}^2$  UV-C and cultured for the indicated times. Levels of unprocessed or cleaved forms of caspase-3 and p53 were measured by Western blotting. **(c)** After  $p53^{-/-}$  HCT116 cells were treated as in **(b)**, numbers of viable cells were counted. The data were normalized by numbers of untreated control cells and expressed as percentages in three independent experiments.

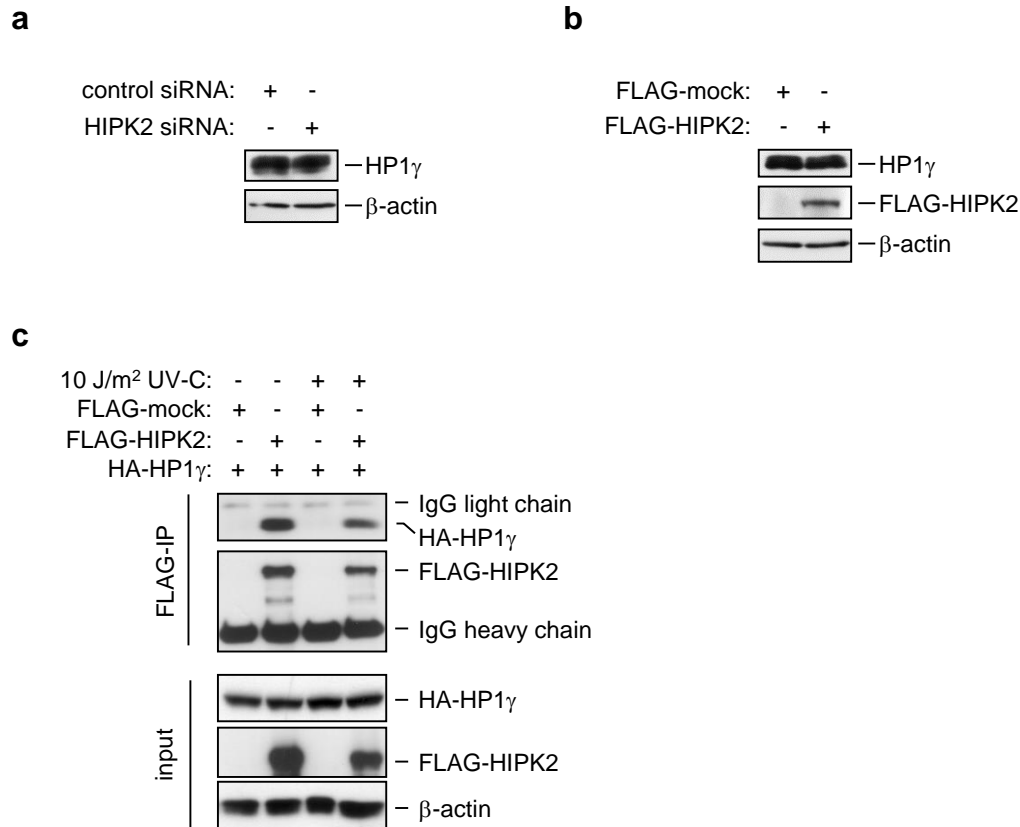
\*Significantly different by unpaired Student's *t*-test ( $P < 0.01$ ).



**Supplementary Figure S4.** Specific association between HIPK2 and HP1 $\gamma$ . **(a)** The scheme of HA-tagged HP1 $\gamma$  lacking the chromo domain (HA- $\Delta$ CD) or the chromo-shadow domain (HA- $\Delta$ CSD). **(b)** HCT116 cells were co-transfected with the FLAG-HIPK2-encoding vector and the vector encoding HA-HP1 $\gamma$ , HA- $\Delta$ CD, or HA- $\Delta$ CSD for 48 h. Amounts of FLAG-HIPK2 and HA-tagged truncated HP1 $\gamma$  in nuclear proteins (input) and immunoprecipitates (FLAG-IP) were measured by Western blotting, with  $\beta$ -actin as a loading control.



**Supplementary Figure S5.** Phosphorylation of HP1γ after 10 J/m<sup>2</sup> UV-C irradiation. **(a)** The amino acid sequence of human HP1γ. Serine and threonine are indicated in bold with an underline. **(b)** HCT116 cells were irradiated with 10 J/m<sup>2</sup> UV-C and incubated for the indicated times. Phosphorylation of HP1γ was detected by phos-tag SDS-PAGE using an anti-HP1γ antibody. **(c)** HCT116 cells were co-transfected with the FLAG-HIPK2-encoding vector and the vector encoding HA-HP1γ, HA-ΔCD, or HA-ΔCSD for 48 h and then irradiated with 10 J/m<sup>2</sup> UV-C. After these cells were cultivated for 12 hours, phosphorylation of HA-HP1γ was detected by phos-tag SDS-PAGE using an anti-HA antibody. **(d)** After HCT116 cells were treated with the vector encoding either FLAG-HIPK2 or FLAG-HIPK2mt2, or an empty vector and then irradiated with 10 J/m<sup>2</sup> UV-C. After cultivation for indicated times, phosphorylation of HP1γ was detected by phos-tag SDS-PAGE using an anti-HP1γ antibody. **(e)** HCT116 cells were treated as described in **(b)**. Changes in the amounts of phosphorylated HP1γ at Ser83 (phospho-HP1γ Ser83) and HP1γ after 10 J/m<sup>2</sup> UV-C irradiation were measured by Western blotting using β-actin as a loading control.



**Supplementary Figure S6.** HIPK2 did not affect expression of HP1 $\gamma$  and UV-C-triggered its binding to HP1 $\gamma$  (a) After HCT116 cells were treated with control or HIPK2 siRNA#1 for 48 h, HP1 $\gamma$  levels were measured by Western blotting, with  $\beta$ -actin as a loading control. (b) After HCT116 cells were transfected with the FLAG-HIPK2-encoding vector or an empty vector for 48 h, amounts of HP1 $\gamma$  and FLAG-HIPK2 levels were measured by Western blotting. (c) HCT116 cells were co-transfected with the FLAG-HIPK2-encoding vector and the vector encoding HA-HP1 $\gamma$  for 48 h and then irradiated with 10 J/m<sup>2</sup> UV-C. After these cells were cultivation for 12 h, amounts of HA-HP1 $\gamma$  in nuclear proteins (input) and immunoprecipitates (FLAG-IP) were measured by Western blotting, with  $\beta$ -actin as a loading control.

**Supplementary Table S1. Antibodies used in this study**

| target proteins                | commercial source         | product number |
|--------------------------------|---------------------------|----------------|
| FLAG-M2                        | Sigma-Aldrich             | F3165          |
| HA -probe (Y-11)               | Santa Cruz Biotechnology  | sc-805         |
| HA -probe (F-7)                | Santa Cruz Biotechnology  | sc-7392        |
| HP1 $\alpha$                   | Cell Signaling Technology | 2616           |
| HP1 $\beta$                    | Abcam (Cambridge, UK)     | ab10478        |
| HP1 $\gamma$                   | Millipore (Billerica, MA) | MAB3450        |
| phospho-HP1 $\gamma$ (Ser83)   | Cell Signaling Technology | 2600           |
| histone H3                     | Abcam                     | ab1791         |
| trimethyl-histone H3 (Lys9)    | Millipore                 | 07-442         |
| phospho-histone H2A.X (Ser139) | Cell Signaling Technology | 2577           |
| phospho-histone H2A.X (Ser139) | Millipore                 | 05-636         |
| p53                            | Cell Signaling Technology | 2527           |
| phospho-p53 (Ser46)            | Cell Signaling Technology | 2521           |
| cleaved caspase-3              | Cell Signaling Technology | 9664           |
| caspase-3                      | Cell Signaling Technology | 9662           |
| cleaved caspase-9              | Cell Signaling Technology | 9501           |
| caspase-9                      | Cell Signaling Technology | 9502           |
| $\beta$ -actin                 | Abcam                     | ab6276         |